Biogeosciences, 15, 4245–4269, 2018
https://doi.org/10.5194/bg-15-4245-2018

Biogeosciences Open Access EGU

Large but decreasing effect of ozone on the European carbon sink

Rebecca J. Oliver[1], **Lina M. Mercado**[1,2], **Stephen Sitch**[2], **David Simpson**[3,4], **Belinda E. Medlyn**[5], **Yan-Shih Lin**[5], **and Gerd A. Folberth**[6]

[1]Centre for Ecology and Hydrology, Benson Lane, Wallingford, OX10 8BB, UK
[2]College of Life and Environmental Sciences, University of Exeter, EX4 4RJ, Exeter, UK
[3]EMEP MSC-W Norwegian Meteorological Institute, PB 43, NO-0313, Oslo, Norway
[4]Dept. Space, Earth & Environment, Chalmers University of Technology, Gothenburg, SE-41296 Sweden
[5]Hawkesbury Institute for the Environment, Western Sydney University, Locked Bag 1797, Penrith NSW 2751 Australia
[6]Met Office Hadley Centre, Exeter, UK

Correspondence: Rebecca Oliver (rfu@ceh.ac.uk)

Received: 28 September 2017 – Discussion started: 11 October 2017
Revised: 17 June 2018 – Accepted: 1 July 2018 – Published: 13 July 2018

Abstract. The capacity of the terrestrial biosphere to sequester carbon and mitigate climate change is governed by the ability of vegetation to remove emissions of CO_2 through photosynthesis. Tropospheric O_3, a globally abundant and potent greenhouse gas, is, however, known to damage plants, causing reductions in primary productivity. Despite emission control policies across Europe, background concentrations of tropospheric O_3 have risen significantly over the last decades due to hemispheric-scale increases in O_3 and its precursors. Therefore, plants are exposed to increasing background concentrations, at levels currently causing chronic damage. Studying the impact of O_3 on European vegetation at the regional scale is important for gaining greater understanding of the impact of O_3 on the land carbon sink at large spatial scales. In this work we take a regional approach and update the JULES land surface model using new measurements specifically for European vegetation. Given the importance of stomatal conductance in determining the flux of O_3 into plants, we implement an alternative stomatal closure parameterisation and account for diurnal variations in O_3 concentration in our simulations. We conduct our analysis specifically for the European region to quantify the impact of the interactive effects of tropospheric O_3 and CO_2 on gross primary productivity (GPP) and land carbon storage across Europe. A factorial set of model experiments showed that tropospheric O_3 can suppress terrestrial carbon uptake across Europe over the period 1901 to 2050. By 2050, simulated GPP was reduced by 4 to 9 % due to plant O_3 damage and land carbon storage was reduced by 3 to 7 %. The combined physiological effects of elevated future CO_2 (acting to reduce stomatal opening) and reductions in O_3 concentrations resulted in reduced O_3 damage in the future. This alleviation of O_3 damage by CO_2-induced stomatal closure was around 1 to 2 % for both land carbon and GPP, depending on plant sensitivity to O_3. Reduced land carbon storage resulted from diminished soil carbon stocks consistent with the reduction in GPP. Regional variations are identified with larger impacts shown for temperate Europe (GPP reduced by 10 to 20 %) compared to boreal regions (GPP reduced by 2 to 8 %). These results highlight that O_3 damage needs to be considered when predicting GPP and land carbon, and that the effects of O_3 on plant physiology need to be considered in regional land carbon cycle assessments.

1 Introduction

The terrestrial biosphere absorbs around 30 % of anthropogenic CO_2 emissions and acts to mitigate climate change (Le Quéré et al., 2015). Early estimates of the European carbon balance suggest a terrestrial carbon sink of between 135 and 205 $TgC\,yr^{-1}$ (Janssens et al., 2003). Schulze et al. (2009) determined a larger carbon sink of 274 $TgC\,yr^{-1}$, and more recent estimates suggest a European terrestrial sink of between 146 and 184 $TgC\,yr^{-1}$ (Luyssaert et al., 2012). The carbon sink capacity of land ecosystems is dominated by the ability of vegetation to sequester carbon through photosynthesis and release it back to the atmosphere through res-

piration. Therefore, any change in the balance of these fluxes will alter ecosystem source–sink behaviour.

In recent decades much attention has focussed on the effects of rising atmospheric CO_2 on vegetation productivity (Ceulemans and Mousseau, 1994; Norby et al., 1999, 2005; Saxe et al., 1998). The Norby et al. (2005) synthesis of Free-Air CO_2 Enrichment (FACE) experiments suggests a median stimulation (23 ± 2 %) of forest net primary production (NPP) in response to a doubling of CO_2. Similar average increases (20 %) were observed for C_3 crops, although this translated into smaller gains in biomass (17 %) and crop yields (13 %) (Long et al., 2006). Little attention, however, has been given to tropospheric ozone (O_3), a globally abundant air pollutant recognised as one of the most damaging pollutants for forests (Karlsson et al., 2007; Royal-Society, 2008; Simpson et al., 2014b). Tropospheric O_3 is a secondary air pollutant formed by photochemical reactions involving carbon monoxide (CO), volatile organic compounds (VOCs), methane (CH_4) and nitrogen oxides (NO_x) from both human-made and natural sources, as well as downward transport from the stratosphere and lightning, which is a source of NO_x. The phytotoxic effects of O_3 exposure are shown to decrease vegetation productivity and biomass, with consequences for terrestrial carbon sequestration (Felzer et al., 2004; Loya et al., 2003; Mills et al., 2011b; Sitch et al., 2007). Few studies, however, consider the simultaneous effects of exposure to both gases, and few Earth system models (ESMs) currently explicitly consider the role of tropospheric O_3 in terrestrial carbon dynamics (IPCC, 2013), both of which are important in understanding the carbon sequestration potential of the land surface and future carbon dynamics regionally and globally (Le Quéré et al., 2016; Sitch et al., 2015).

Due to increased anthropogenic precursor emissions over the industrial period, background concentrations of ground-level O_3 have risen (Vingarzan, 2004). Background O_3 is generally defined as the O_3 pollution present in a region that is not attributed to local anthropogenic sources (Vingarzan, 2004). O_3 levels at the start of the 20th century are estimated to be around 10 ppb for the Montsouris Observatory site near Paris, data for Arkona on the Baltic coast increased from ca. 15 ppb in the 1950s to 20–27 ppb by the early 1980s, and the Irish coast site Mace Head shows around 40 ppb by the year 2000 (Logan et al., 2012; Parrish et al., 2012). Present-day annual average background O_3 concentrations reported in the review of Vingarzan (2004) show O_3 concentrations range between approximately 20 and 45 ppb, with the greatest increase occurring since the 1950s. Trends vary from site to site though, even on a decadal basis (Logan et al., 2012; Simpson et al., 2014b), depending, for example, on local/regional trends in precursor (especially NO_x) emissions, elevation and exposure to long-range transport of O_3. Nevertheless, there is some indication that background O_3 levels over the mid-latitudes of the Northern Hemisphere have continued to rise at a rate of approximately 0.5–2 % per year, although not uniformly (Vingarzan, 2004). As a result of controls on precursor emissions in Europe and North America, peak O_3 concentrations in these regions have decreased or stabilised over recent decades (Cooper et al., 2014; Logan et al., 2012; Parrish et al., 2012; Simpson et al., 2014b). Nevertheless, climate change may increase the frequency of weather events conducive to peak O_3 incidents in the future (e.g. summer droughts and heatwaves; Sicard et al., 2013), and may increase biogenic emissions of the O_3 precursors isoprene and NO_x, although such impacts are subject to great uncertainty (Simpson et al., 2014b; Young et al., 2009, 2013). Intercontinental transport of air pollution from regions such as Asia are thought to contribute substantially to rising background O_3 concentrations over the last decades (Cooper et al., 2010; Verstraeten et al., 2015). Northern Hemisphere background concentrations of O_3 are now close to established levels for impacts on human health and the terrestrial environment (Royal-Society, 2008). Therefore, although peak O_3 concentrations are in decline across Europe, plants are exposed to increasing background levels, at levels currently causing chronic damage (Mills et al., 2011b). Intercontinental transport means future O_3 concentrations in Europe will be partly dependent on how O_3 precursor emissions evolve globally (Auvray and Bey, 2005; Derwent et al., 2015).

Rising background O_3 concentrations impact agricultural yields and nutritional quality of major crops (Ainsworth et al., 2012; Avnery et al., 2011), with consequences for global food security (Tai et al., 2014). Increasing background levels of O_3 are damaging to ecosystem health and reduce the global land carbon sink (Arneth et al., 2010; Sitch et al., 2007). Reduced uptake of carbon by plant photosynthesis due to O_3 damage allows more CO_2 to remain in the atmosphere. This effect of O_3 on plant physiology represents an additional climate warming to the direct radiative forcing of O_3, a potent greenhouse gas (Collins et al., 2010; Sitch et al., 2007), the magnitude of which, however, remains highly uncertain (IPCC, 2013).

Dry deposition of O_3 to terrestrial surfaces, primarily uptake by stomata on plant foliage and deposition on external surfaces of vegetation (Fowler et al., 2001, 2009), is a large sink for ground-level O_3 (Wild, 2007; Young et al., 2013). On entry to sub-stomatal spaces, O_3 reacts with other molecules to form reactive oxygen species (ROS). Plants can tolerate a certain level of O_3 depending on their capacity to scavenge and detoxify the ROS (Ainsworth et al., 2012). Above this critical level, long-term chronic O_3 exposure reduces plant photosynthesis and biomass accumulation (Ainsworth, 2008, 2012; Matyssek et al., 2010a; Wittig et al., 2007, 2009), either directly through effects on photosynthetic machinery such as reduced Rubisco content (Ainsworth et al., 2012; Wittig et al., 2009) and/or indirectly by reduced stomatal conductance (g_s) (Kitao et al., 2009; Wittig et al., 2007), alters carbon allocation to different pools (Grantz et al., 2006; Wittig et al., 2009), accelerates leaf senescence (Ainsworth,

2008; Nunn et al., 2005; Wittig et al., 2009) and changes plant susceptibility to biotic stress factors (Karnosky et al., 2002; Percy et al., 2002).

The response of plants to O_3 is very wide-ranging as reported in the literature from different field studies. The Wittig et al. (2007) meta-analysis of temperate and boreal tree species showed that raised O_3 concentrations significantly reduced leaf-level light-saturated net photosynthetic uptake (-19 %, range: -3 to -28 % at a mean O_3 concentration of 85 ppb) and g_s (-10 %, range: $+5$ to -23 % at a mean O_3 concentration of 91 ppb) in both broadleaf and needleleaf tree species. In the Feng et al. (2008) meta-analysis of wheat, O_3 reduced aboveground biomass (-18 % at a mean O_3 concentration of 70 ppb) photosynthetic rate (-20 % at a mean O_3 concentration of 73 ppb) and g_s (-22 % at a mean O_3 concentration of 79 ppb). One of few long-term field-based O_3 exposure studies (AspenFACE) showed that after 11 years of exposing mature trees to O_3 (mean O_3 concentration of 46 ppb), O_3 decreased ecosystem carbon content (-9 %) and decreased NPP (-10 %), although the O_3 effect decreased through time (Talhelm et al., 2014). Zak et al. (2011) showed this was partly due to a shift in community structure as O_3-tolerant species, competitively inferior in low-O_3 environments, outcompeted O_3-sensitive species. Gross primary productivity (GPP) was reduced (-12 to -19 %) at two Mediterranean ecosystems exposed to O_3 (ranging between 20 and 72 ppb across sites and through the year) studied by Fares et al. (2013). Biomass of mature beech trees was reduced (-44 %) after 8 years of exposure to O_3 (~ 150 ppb) (Matyssek et al., 2010a). After 5 years of O_3 exposure (ambient $+20$ to $+40$ ppb) in a semi-natural grassland, annual biomass production was reduced (-23 %), and in a Mediterranean annual pasture O_3 exposure significantly reduced total aboveground biomass (up to -25 %) (Calvete-Sogo et al., 2014). However, these were empirical studies at individual sites, and these focus on O_3 effects on plant physiology and productivity but do not quantify the impact on the land carbon sink. Modelling studies are needed to scale site observations to the regional and global scales. Models generally suggest that plant productivity and carbon sequestration will decrease with O_3 pollution, though the magnitudes vary. For example, based on a limited dataset to parameterise plant O_3 damage for a global set of plant functional types (PFTs), Sitch et al. (2007) predicted a decline in global GPP of 14 to 23 % by 2100. A second study by Lombardozzi et al. (2015) predicted a 10.8 % decrease in present-day (2002–2009) GPP globally. Here we take a regional approach and take advantage of the latest measurements showing changes in plant productivity with accumulated exposure to O_3 specifically for a range of European vegetation from different regions (CLRTAP, 2017) with which to calibrate the JULES model for plant sensitivity to O_3, and we conduct our analysis specifically for the European region.

Understanding the response of plants to elevated tropospheric O_3 is challenged by the large variation in O_3 sensitivity both within and among species (Karnosky et al., 2007; Kubiske et al., 2007; Wittig et al., 2009). Additionally, other environmental stresses that affect stomatal behaviour will affect the rate of O_3 uptake and therefore the response to O_3 exposure, such as high temperature, drought and changing concentrations of atmospheric CO_2 (Mills et al., 2016; Fagnano et al., 2009; Kitao et al., 2009; Löw et al., 2006). Increasing concentrations of atmospheric CO_2, for example, are suggested to provide some protection against O_3 damage by causing stomata to close (Harmens et al., 2007; Wittig et al., 2007); however the long-term effects of CO_2 fertilisation on plant growth and carbon storage remain uncertain (Baig et al., 2015; Ciais et al., 2013). Further, in some studies, stomata have been shown to respond sluggishly, losing their responsiveness to environmental stimuli with exposure to O_3, which can lead to higher O_3 uptake, increased water loss and therefore greater vulnerability to environmental stresses such as drought (Mills et al., 2009, 2016; Paoletti and Grulke, 2010; Wilkinson and Davies, 2009).

Given the critical role g_s plays in the uptake of both CO_2 and O_3, we use an alternative representation and parameterisation of g_s in JULES by implementing the Medlyn et al. (2011) g_s formulation. This model is based on the optimal theory of stomatal behaviour and has advantages over the current JULES g_s formulation of Jacobs (1994) including (i) a single parameter (g_1) compared to two parameters in Jacobs (1994), (ii) the g_1 parameter is related to the water-use strategy of vegetation and is easier to parameterise with commonly measured leaf- or canopy-level observations of photosynthesis, g_s, and humidity, and (iii) values of g_1 are available for many different PFTs derived from a global dataset of leaf-level measurements (Lin et al., 2015).

The main objective of this work is to assess the impact of historical and projected (1901 to 2050) changes in tropospheric O_3 and atmospheric CO_2 concentration on predicted GPP and the land carbon sink for Europe. These are the two greenhouse gases that directly affect plant photosynthesis and g_s. We use a factorial suite of model experiments, using the Joint UK Land Environment Simulator (JULES) (Best et al., 2011; Clark et al., 2011) and the land surface model of the UK Earth System Model (UKESM) (Collins et al., 2011) to simulate plant O_3 uptake and damage and to investigate the impact of both O_3 and CO_2 on plant water use and carbon uptake. In this work, the JULES model is recalibrated using the latest observations of vegetation sensitivity to O_3, with the addition of a separate parameterisation for temperate and boreal regions versus the Mediterranean. The O_3 sensitivity of each PFT in JULES was recalibrated for both a high and low sensitivity to account for uncertainty in the O_3 response, in part due to the observed variation in O_3 sensitivity among species. This includes O_3 sensitivities for agricultural crops (wheat – high sensitivity) versus natural grassland (low sensitivity), with separate sensitivities for Mediterranean grasslands. For forests JULES is parameterised with O_3 sensitivities for broadleaf and needleleaf trees (with a high and low

O_3 sensitivity for both), with separate sensitivities (high and low) for Mediterranean broadleaf species. We make a separate distinction for the Mediterranean region where possible because the work of Büker et al. (2015) showed that the sensitivity of dominant Mediterranean trees to O_3 is different from temperate species. In addition, we introduce an alternative g_s scheme into JULES as described above. JULES is forced with spatially varying daily O_3 concentrations from a high-resolution atmospheric chemistry model for Europe that are disaggregated to hourly concentrations; therefore our simulations account for diurnal variations in O_3 concentration and O_3 responses, allowing for improved estimates of O_3 uptake by vegetation. We do not attempt to make a full assessment of the carbon cycle of Europe, instead we target O_3 damage, which is currently a missing component in earlier carbon cycle assessments (Le Quéré et al., 2018; Sitch et al., 2015). To this end, we prescribe changing O_3 and CO_2 concentrations from 1901 to 2050 but using a fixed pre-industrial climate. We acknowledge the use of a "fixed" pre-industrial climate omits the additional uncertainty of the interaction between climate change and g_s, which will affect the rate of O_3 uptake and therefore O_3 concentrations. In addition, using uncoupled chemistry and climate is a further source of uncertainty. To understand the impact of these complex feedback mechanisms is an important area for future work, but in the current study our aim is to isolate the physiological response of plants to both O_3 and CO_2 and determine the sensitivity of predicted GPP and the land carbon sink to this process, as the impact of O_3 on the land carbon sink currently remains largely unknown at large spatial scales for Europe.

2 Methods

2.1 Representation of O_3 effects in JULES

JULES calculates the land–atmosphere exchanges of heat, energy, mass, momentum and carbon on a sub-daily time step, and includes a dynamic vegetation model (Best et al., 2011; Clark et al., 2011; Cox, 2001). This work uses JULES version 3.3 (http://www.jchmr.org, last access: 10 September 2017) at a $0.5^\circ \times 0.5^\circ$ spatial resolution and hourly model time step; the spatial domain is shown in Fig. S1 in the Supplement. JULES has a multilayer canopy radiation interception and photosynthesis scheme (10 layers in this instance) that accounts for direct and diffuse radiation, sun fleck penetration through the canopy, inhibition of leaf respiration in the light and change in photosynthetic capacity with depth into the canopy (Clark et al., 2011; Mercado et al., 2009). Soil water content also affects the rate of photosynthesis and g_s. It is modelled using a dimensionless soil water stress factor, β, which is related to the mean soil water concentration in the root zone, and the soil water contents at the critical and wilting points (Best et al., 2011).

To simulate the effects of stomatal O_3 deposition on vegetation productivity and water use, JULES uses the flux-gradient approach of Sitch et al. (2007), modified to include non-stomatal deposition following Tuovinen et al. (2009). A similar approach is taken by Franz et al. (2017) in the OCN model; however plant O_3 damage is a function of accumulated O_3 exposure over time. In JULES, plant O_3 damage is instantaneous because the impact of cumulative O_3 exposure on plant productivity has already been calibrated with observations (described below). JULES uses a coupled model of g_s and photosynthesis; the potential net photosynthetic rate (A_p, mol CO_2 m^{-2} s^{-1}) is modified by an "O_3 uptake" factor (F the fractional reduction in photosynthesis), so that the actual net photosynthesis (A_{net}, mol CO_2 m^{-2} s^{-1}) is given by Eq. (1) (Clark et al., 2011; Sitch et al., 2007). Because of the relationship between these two fluxes, the direct effect of O_3 damage on photosynthetic rate also leads to a reduction in g_s. An alternative approach was taken by Lombardozzi et al. (2012) in the CLM model in which photosynthesis and g_s are decoupled, so that O_3 exposure affects carbon assimilation and transpiration independently. In JULES, changes in atmospheric CO_2 concentration also affect photosynthetic rate and g_s; consequently the interactive effects of changing concentrations of both CO_2 and O_3 are allowed for.

$$A_{net} = A_p F \tag{1}$$

The O_3 uptake factor (F) is defined as

$$F = 1 - a \cdot \max\left[F_{O_3} - F_{O_3 crit}, 0.0\right]. \tag{2}$$

F_{O_3} is the instantaneous leaf uptake of O_3 (nmol m^{-2} s^{-1}), $F_{O_3 crit}$ is a PFT-specific threshold for O_3 damage (nmol m^{-2} PLA s^{-1}, projected leaf area) and "a" is a PFT-specific parameter representing the fractional reduction of photosynthesis with O_3 uptake by leaves. Following Tuovinen et al. (2009), the flux of O_3 through stomata, $F_{O_3 crit}$, is represented as follows:

$$F_{O_3} = O_3 \left(\frac{g_b \left(\frac{g_l}{K_{O_3}}\right)}{g_b + \left(\frac{g_l}{K_{O_3}}\right) + g_{ext}} \right). \tag{3a}$$

O_3 is the molar concentration of O_3 at reference (canopy) level (nmol m^{-3}), g_b is the leaf-scale boundary layer conductance (m s^{-1}, Eq. 3b), g_l is the leaf conductance for water (m s^{-1}), K_{O_3} accounts for the different diffusivity of ozone to water vapour and takes a value of 1.51 after Massman (1998), and g_{ext} is the leaf-scale non-stomatal deposition to external plant surfaces (m s^{-1}), which takes a constant value of 0.0004 m s^{-1} after Tuovinen et al. (2009). The leaf-level boundary layer conductance (g_b) is calculated as in Tuovinen et al. (2009).

$$g_b = \alpha \mathrm{Ld}^{-1/2} U^{-1/2} \tag{3b}$$

α is a constant (0.0051 m $s^{-1/2}$), Ld is the cross-wind leaf dimension (m) defined per PFT as 0.05 for trees, 0.02 for

grasses (C_3 and C_4), and 0.04 for shrubs and U is wind speed at canopy height ($m\,s^{-1}$). The rate of O_3 uptake is dependent on g_s, which is dependent on photosynthetic rate. Given g_s is a linear function of photosynthetic rate in JULES (Clark et al., 2011), from Eq. (1) it follows that

$$g_s = g_1 F. \quad (4)$$

The O_3 flux to stomata, F_{O_3}, is calculated at leaf level and then scaled to each canopy layer differentiating sunlit and shaded leaf photosynthesis, and is finally summed up to the canopy level. Because the photosynthetic capacity, photosynthesis and therefore g_s decline with depth into the canopy, this in turn affects O_3 uptake, with the top leaf level contributing most to the total O_3 flux and the lowest level contributing least.

2.2 Calibration of O_3 uptake model

Here we use the latest literature on flux-based O_3 dose–response relationships derived from observed field data across Europe (CLRTAP, 2017) to determine the key PFT-specific O_3 sensitivity parameters in JULES (a and F_{O_3crit}). Synthesis of information expressed as O_3 flux-based dose–response relationships derived from field experiments is carried out by the United Nations Convention on Long-Range Transboundary Air Pollution (CLRTAP), this information is then used as a policy tool to inform emission reduction strategies in Europe to improve air quality (CLRTAP, 2017; Mills et al., 2011a). Derivation of O_3 flux-based dose–response relationships for different vegetation types uses the accumulated stomatal O_3 flux above a threshold (often referred to as the phytotoxic O_3 dose above a threshold of "y" i.e. POD_y) as the dose metric, and the percentage change in biomass as the response metric (Emberson et al., 2007; Karlsson et al., 2007). We use these observation-based O_3 dose–response relationships to calibrate each JULES PFT for sensitivity to O_3 using available relationships for the closest matching vegetation type. For JULES, F_{O_3crit} is the threshold for O_3 damage, and values for this parameter are taken from the O_3 dose–response relationships as the POD_y value (see CLRTAP, 2017, and Büker et al., 2015, for derivation of POD_y values). The actual sensitivity to O_3 is determined by the slope of the O_3 dose–response relationship, i.e. how much biomass changes with accumulated stomatal uptake of O_3 above the damage threshold; this relates to the parameter a in JULES. The parameter a is a PFT-specific parameter representing the fractional reduction of photosynthesis with O_3 uptake by leaves. Values for this parameter are found for each PFT by running JULES with different values of a, which alter the instantaneous photosynthetic rate, but then calculating the accumulated stomatal flux of O_3 and the change in productivity until the slope of this relationship produced by the JULES simulations matches that of the O_3 dose–response relationships derived from observations. Essentially we calibrate each JULES PFT for sensitivity to O_3 by reproducing the observation-based O_3 dose–response relationships.

Each PFT was calibrated for high and low plant O_3 sensitivity to account for uncertainty in the sensitivity of different plant species to O_3, using the approach of Sitch et al. (2007). Therefore, when using our results to assess the impact of O_3 at the land surface, we are able to provide a range in our estimates to help address some of the uncertainty in the O_3 response of different vegetation types. In addition, where possible owing to available data, a distinction was made for Mediterranean regions. This was because the work of Büker et al. (2015) showed that different O_3 dose–response relationships are needed to describe the O_3 sensitivity of dominant Mediterranean trees. For the C_3 herbaceous PFT, the dominant land cover type across the European domain in this study (Fig. S2), the high plant O_3 sensitivity was calibrated against observations for wheat to give a representation of agricultural regions and wheat is one of the most sensitive grasses to O_3 (Fig. S3, Table S1). For the low plant O_3 sensitivity JULES was calibrated against the dose–response function for natural grassland to give a representation of natural grassland and this vegetation has a much lower sensitivity to O_3 damage; for the Mediterranean region we used a function for Mediterranean natural grasslands, all taken from CLRTAP (2017) (Fig. S3, Table S1 in the Supplement). Tree–shrub PFTs were calibrated against observed O_3 dose–response functions for the high plant O_3 sensitivity: broadleaf trees (temperate–boreal): birch–beech dose–response relationship; broadleaf trees (Mediterranean): deciduous oak dose–response relationship; needleleaf trees: Norway spruce dose–response relationship; shrubs: birch–beech dose–response relationship; all from CLRTAP (2017) (Fig. S3, Table S1). Data on O_3 dose–response relationships for different vegetation types is very limited; therefore for the low plant O_3 sensitivity calibration for trees–shrubs we assumed a 20 % decrease in sensitivity to O_3 based on the difference in sensitivity between high- and low-sensitivity tree species in the Karlsson et al. (2007) study. Due to limitations in data availability, the shrub parameterisation uses the observed dose–response functions for broadleaf trees. Similarly, the parameterisation for C_4 herbaceous uses the observed dose–responses for C_3 herbaceous; however the fractional cover of C_4 herbs across Europe is low (Fig. S2), so this assumption affects a very small percentage of land cover.

To calibrate the JULES O_3 uptake model, JULES was run across Europe forced using the WFDEI observational climate dataset (Weedon, 2013) at $0.5° \times 0.5°$ spatial and 3 h temporal resolution. JULES uses interpolation to disaggregate the forcing data down from 3 h to an hourly model time step. The model was spun up over the period from 1979 to 1999 with a fixed atmospheric CO_2 concentration of 368.33 ppm (1999 value from Mauna Loa observations; Tans and Keeling, 2014). Zero tropospheric ozone concentration was assumed for the control simulation. For the simulations with O_3, spin-up used spatially explicit fields of present-day O_3

concentration produced using the UK Chemistry and Aerosol (UKCA) model with standard chemistry from the run evaluated by O'Connor et al. (2014). A fixed land cover map was used based on IGBP (International Geosphere-Biosphere Programme) land cover classes (IGBP-DIS). Therefore as the vegetation distribution was fixed and the calibration was not looking at carbon stores, a short spin-up time was adequate to equilibrate soil temperature and soil moisture. JULES was then run for the year 2000 with a corresponding CO_2 concentration of 369.52 ppm (from Mauna Loa observations; Tans and Keeling, 2014) and monthly fields of spatially explicit tropospheric O_3 (O'Connor et al., 2014) as necessary.

Calibration was performed using four simulations: with (i) zero tropospheric O_3 concentration, as the control simulation (control), (ii) tropospheric O_3 at the current ambient concentration (O_3), (iii) ambient +20 ppb ($O_3 + 20$) and (iv) ambient +40 ppb ($O_3 + 40$). The different O_3 simulations (i.e. O_3, $O_3 + 20$ and $O_3 + 40$) were used to capture the range of O_3 conditions in the data used in the observation-based O_3 dose–response relationships used in this study for calibration. Often data were from experiments using artificially manipulated conditions of ambient +40 ppb O_3, for example. For each JULES O_3 simulation, the value of $F_{O_3 crit}$ was taken from the vegetation-specific O_3 dose–response relationship as the threshold O_3 concentration above which damage to vegetation occurs. An initial estimate of the parameter a was used. Then for each PFT and each simulation, hourly estimates of NPP (our proxy for biomass – although not identical, they are related) and O_3 uptake in excess of $F_{O_3 crit}$ were accumulated over a PFT-dependent accumulation period. The accumulation periods were ~ 6 months for broadleaf trees and shrubs, all year for needleleaf trees and ~ 3 months for herbaceous species, through the growing season, following guidelines in CLRTAP (2017). Additionally, in accordance with the methods used in CLRTAP (2017) that describe how the O_3 dose–response relationships are derived from observations, we use the stomatal O_3 flux per projected leaf area to top canopy sunlit leaves. The percentage change in total NPP was calculated for each O_3 simulation and plotted against the cumulative uptake of O_3 over the PFT-specific accumulation period. The linear regression of this relationship was calculated, and slope and intercept were compared against the slope and intercept of the observed dose–response relationships. Values of the parameter a were adjusted, and the procedure was repeated until the linear regression through the simulation points matched that of the observations (Fig. S3, Table S1).

2.3 Representation of stomatal conductance and site-level evaluation

In JULES, g_s ($m\,s^{-1}$) is represented following the closure proposed by Jacobs (1994):

$$g_s = 1.6 R T_l \frac{A_{net}\beta}{c_a - c_i}. \quad (5)$$

In this parameterisation, c_i is unknown and in the default JULES model is calculated as in Eq. (6), hereafter called JAC:

$$c_i = (c_a - c_*)\, f_0 \left(1 - \frac{dq}{dq_{crit}}\right) + c_*. \quad (6)$$

β is a soil moisture stress factor, the factor 1.6 accounts for g_s being the conductance for water vapour rather than CO_2, R is the universal gas constant ($J\,K^{-1}\,mol^{-1}$), T_l is the leaf surface temperature (K), c_a and c_i (both Pa) are the leaf surface and internal CO_2 partial pressures, respectively, c_* (Pa) is the CO_2 photorespiration compensation point, dq is the humidity deficit at the leaf surface ($kg\,kg^{-1}$), dq_{crit} ($kg\,kg^{-1}$) and f_0 are PFT-specific parameters representing the critical humidity deficit at the leaf surface, and the leaf internal-to-atmospheric CO_2 ratio (c_i/c_a) at the leaf specific humidity deficit (Best et al., 2011); values are shown in Table S1.

In this work, we replace Eq. (6) with the closure described in Medlyn et al. (2011), using the key PFT-specific model parameter g_1 ($kPa^{0.5}$), and dq is expressed in kilopascals, shown in Eq. (7), hereafter called MED:

$$c_i = c_a \left(\frac{g_1}{g_1 + \sqrt{dq}}\right). \quad (7)$$

PFT-specific values of the g_1 parameter were derived for European vegetation from the database of Lin et al. (2015) and are shown in Table S1. The g_1 parameter represents the sensitivity of g_s to the assimilation rate, i.e. plant water use efficiency, and was derived as in Lin et al. (2015) by fitting the Medlyn et al. (2011) model to observations of g_s, photosynthesis, and vapour pressure deficit (VPD), assuming an intercept of zero.

The impact of g_s model formulation (JAC versus MED) on simulated water, O_3, carbon and energy fluxes is compared for two contrasting grid points – wet (low soil moisture stress) and dry (high soil moisture stress) in the European domain. JULES was spun up for 20 years (1979–1999) at two grid points in central Europe representing a wet (low soil moisture stress; lat: 48.25, long: 5.25) and a dry site (high soil moisture stress; lat: 38.25, long: −7.75). The modelled soil moisture stress factor (fsmc) at the wet site ranged from 0.8 to 1.0 over the year 2000 (1.0 indicates no soil moisture stress), and at the dry site fsmc steadily declined from 0.8 at the start of the year to 0.25 by the end of the summer. The WFDEI meteorological forcing dataset (Weedon, 2013), along with atmospheric CO_2 concentration for the year 1999 (368.33 ppm), was used and either no O_3 (i.e. the O_3 damage model was switched off) for the control simulations or spatially explicit fields of present-day O_3 concentration produced using the UK Chemistry and Aerosol (UKCA) model from the run evaluated by O'Connor et al. (2014) for the simulations with O_3 were used. Following the spin-up period, JULES was run for 1 year (2000) with corresponding atmospheric CO_2 concentration, and tropospheric O_3 con-

centrations as described above. The control and O_3 simulations were performed for both JAC and MED model formulations. Land cover for the spin-up and main run was fixed at 20 % for each PFT. For the simulations including O_3 damage, the high plant O_3 sensitivity parameterisation was used. The difference between these simulations was used to assess the impact of g_s model formulation on the leaf-level fluxes of carbon and water. We calculate and report (results Sect. 3.1) the difference in mean annual water use that results from the above simulations using the different g_s models. For each day of the simulation we calculate the percentage difference in water use between the two simulations; we then calculate the mean and standard deviation over the year to give the annual mean leaf-level water use.

Site-level evaluation of the two g_s models compared to FLUXNET observations was carried out to evaluate the seasonal cycles of latent and sensible heat using the two g_s models JAC and MED compared to observations. Seven FLUXNET towers were selected to represent a range of land cover types as shown in Table S2. JULES was set up for each site using observed site-level hourly meteorology, and the vegetation cover was prescribed according to the fractional covers of the different JULES surface types shown in Table S2. Following a spin-up period, simulations were run at each site for the years shown in Table S2.

2.4 Model simulations for Europe

2.4.1 Forcing datasets

We used the WATCH meteorological forcing dataset (Weedon et al., 2010, 2011) at 0.5° × 0.5° spatial and 3 h temporal resolution for our JULES simulations. JULES interpolates this down to an hourly model time step. For this study, the climate was kept constant by recycling over the period from 1901 to 1920 to allow us to focus on the impact of O_3, CO_2 and their interactive effects.

JULES was run with prescribed annual mean atmospheric CO_2 concentrations. Pre-industrial global CO_2 concentrations for 1900 to 1960 were taken from Etheridge et al. (1996), for 1960 to 2002 were from Mauna Loa (Keeling and Whorf, 2004), as calculated by the Global Carbon Project (Le Quéré et al., 2016), and for 2003–2050 were based on the IPCC SRES A1B scenario and were linearly interpolated to gap-fill missing years (Fig. 1).

JULES was run including dynamic vegetation with a land cover mask giving the fraction of agriculture in each 0.5° × 0.5° grid cell based on the Hurtt et al. (2011) land cover database for the year 2000. The agricultural mask is fixed and does not change over the simulation period. This means that whilst the model is allowed to evolve its own vegetation cover outside of the agricultural mask, within the mask only C_3 and C_4 herbaceous PFTs are allowed to grow, with no competition from other PFTs. Therefore, through the simulation period, regions of agriculture are maintained as

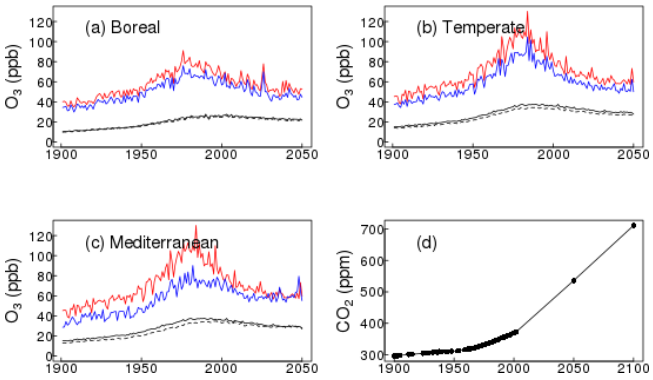

Figure 1. Regional time series of canopy height O_3 (ppb) forcing from EMEP **(a–c)** and **(d)** global atmospheric CO_2 (ppm) concentration (this does not vary regionally; black dots show data points; the black line shows interpolated points). Each panel for the O_3 forcing shows the regional annual average (woody PFTs, black solid line; herbaceous PFTs, black dashed line) and the annual maximum O_3 concentration above: woody PFTs (red) and herbaceous PFTs (blue).

such and not outcompeted by forests, for example, allowing for a more accurate representation of the land cover of Europe in the model. No form of land management is simulated (i.e. no crop harvesting, ploughing, rotation or grazing); growth and leaf area index (LAI) are determined by resource availability and phenology. Outside of the agricultural mask, dynamic vegetation means that grid cell PFT coverage and LAI are the result of resource availability, phenology and simulated competition. Across the model domain, simulated mean annual LAI was dominantly within the range of 2 to 5 $m^2\ m^{-2}$ (Figs. S4 and S5). Following a full spin-up period (to ensure equilibrium vegetation, carbon and water states), there was no significant change in the fractional cover of each PFT over the simulation period (1901–2050). By 2050, increases in boreal forest cover occurred, but this was less than 2 % and limited to very small areas; given this small change we show just the land cover for 2050 in Fig. S2.

Tropospheric O_3 concentration was produced by the EMEP MSC-W model at 0.5° × 0.5° resolution (Simpson et al., 2012), driven with meteorology from the regional climate model RCA3 (Kjellström et al., 2011; Samuelsson et al., 2011), which provides a downscaling of ECHAM A1B-r3 (simulation 11 of Kjellström et al., 2011). This set-up (EMEP + RCA3) is also used by Langner et al. (2012a), Simpson et al. (2014a), Tuovinen et al. (2013), Franz et al. (2017) and Engardt et al. (2017), in which further details and model evaluation can be found. Unfortunately, the three-dimensional RCA3 data needed by the EMEP model were not available prior to 1960, but as in Engardt et al. (2017) the meteorology of 1900–1959 had to be approximated by assigning random years from 1960 to 1969. This procedure introduces some uncertainty of course, although Langner et al. (2012b) show that for the period from 1990 to 2100 it

is emissions change, rather than meteorological change, that drives modelled O_3 concentrations. The emissions scenarios for 1900–2050 merge data from the International Institute of Applied System Analysis (IIASA) for 2005–2050 (the so-called ECLIPSE 4a scenario), recently revised EMEP data for 1990 and a scaling back from 1990 to 1900 using data from Lamarque et al. (2013). The trend in emissions of the major O_3 precursors NO_x, non-methane volatile organic compounds (NMVOCs) and isoprene are shown from 1900 to 2050 over Europe in Fig. S6. Isoprene emissions are not inputs to the EMEP model, but rather calculated at each time step using temperature, radiation and land-cover-specific emission factors (Simpson et al., 2012). Changes in the assumed background concentration of CH_4 (from RCP6.0) (van Vuuren et al., 2011) are also shown in Fig. S6. Engardt et al. (2017) show the trend in emissions of SO_2 and NH_3 from 1900 to 2050 over Europe. The EMEP model accounts for changes in biogenic volatile organic compound (BVOC) emissions as a result of predicted ambient temperature changes.

O_3 concentrations from EMEP MSC-W were calculated at canopy height for two land cover categories: forest and grassland (Figs. S7 and S8), which are taken as surrogates for high and low vegetation, respectively. These canopy-height-specific concentrations allow for the large gradients in O_3 concentration that can occur in the lowest tens of metres, giving lower O_3 for grasslands than seen at 20 m in a forest canopy, for example (Gerosa et al., 2017; Simpson et al., 2012; Tuovinen et al., 2009). These canopy-level O_3 concentrations are used as input to JULES, using the EMEP O_3 concentrations for forest for the forest JULES PFTs (broadleaf or needleleaf, tree and shrub), and the EMEP O_3 concentrations for grassland for the grass–herbaceous JULES PFTs (C_3 and C_4). This study used daily mean values of tropospheric O_3 concentration from EMEP disaggregated down to the hourly JULES model time step. The daily mean O_3 forcing was disaggregated to follow a mean diurnal profile of O_3, which was generated from hourly O_3 output from EMEP MSC-W for the two land cover categories (forest and grassland as described above) across the same model domain. O_3 concentrations follow a diurnal cycle and peak during the day; therefore accounting for the diurnal variation in O_3 concentrations allows for a more realistic estimation of O_3 uptake.

Figure 1 shows large increases in tropospheric O_3 from pre-industrial to present day (2001), which is in line with modelling studies (Young et al., 2013) and site observations (Derwent et al., 2008; Logan et al., 2012; Parrish et al., 2012), and is predominantly a result of increasing anthropogenic emissions (Young et al., 2013). Figures S7 and S8 show this large increase in ground-level O_3 concentrations from 1901 to 2001 occurs in all seasons. Present-day O_3 concentration shows a strong seasonal cycle, with a spring–summer peak in concentrations in the mid-latitudes of the Northern Hemisphere (Derwent et al., 2008; Parrish et al., 2012; Vingarzan, 2004). Seasonal cycles have been changing over the past decades, however, attributed to changes in NO_x and other emissions, as well as changes in transport patterns (Parrish et al., 2013). These changes will likely continue in the future as emissions and meteorological factors impact photochemical O_3 production and transport patterns. Indeed, the O_3 concentrations used in the simulations in this study show increased O_3 levels in winter and in some regions in autumn and spring in 2050 compared to present day, which may be due to reduced titration of O_3 by NO as a result of reduced NO_x emissions in the future (Royal Society, 2008). Summer O_3 concentrations are lower in 2050, however, compared to 2001.

2.4.2 Spin-up and factorial experiments

JULES was spun up by recycling the climate from the early part of the twentieth century (1901 to 1920) using atmospheric CO_2 (296.1 ppm) and O_3 concentrations from 1901 (Figs. S7 and S8). Model spin-up was 2000 years by which point the carbon pools and fluxes were in steady state with zero mean net land–atmosphere CO_2 flux. We performed the following transient simulations for the period from 1901 to 2050 with continued recycling of the climate as used in the spin-up, for both high and low plant O_3 sensitivities:

- run_O_3: fixed 1901 CO_2, varying O_3;
- run_CO_2: varying CO_2, fixed 1901 O_3;
- run_both_CO_2+O_3: varying CO_2, varying O_3.

We use these simulations to investigate the direct effects of changing atmospheric CO_2 and O_3 concentrations, individually and combined, on plant water use, GPP and the land C sink through the twentieth century and into the future, specifically over three time periods: historical (1901–2001), future (2001–2050) and over the full time series (1901–2050). For each time period we calculate the difference between the decadal means calculated at the start and end of the analysis period for each variable of interest. Therefore our results report the change in GPP, for example, over the analysis period. For each variable analysed (GPP, NPP, vegetation carbon, soil carbon, total land carbon and g_s), we use the mean over 10 years to represent each time period, e.g. the mean over 2040 to 2050 is what we call 2050, and 1901 to 1910 is what we refer to as 1901. The difference among the simulations gives the effect of O_3 and CO_2 either separately or in combination over the different time periods. We look at the percentage change due to either O_3 at pre-industrial CO_2 concentration (i.e. without the additional effect of atmospheric CO_2 on stomatal behaviour – run_O_3), CO_2 (at fixed pre-industrial O_3 concentration, run_CO_2) or the combined effect of both gases (run_both_CO_2+O_3), e.g. $100 \cdot (\mathrm{var}O_3[2050] - \mathrm{var}O_3[1901])/\mathrm{var}O_3[1901]$ gives the O_3 effect (at fixed CO_2) over the full experimental period. The meteorological forcing is prescribed in these simulations and is therefore the same among the model runs. Other climate

factors, such as VPD, temperature and soil moisture availability are accounted for in our simulations, but our analysis isolates the effects of O_3, CO_2 and $O_3 + CO_2$. We also use a paired t test to determine statistically significant differences between the different (high and low) plant O_3 sensitivities.

2.4.3 Evaluation

To evaluate our JULES simulations we compare mean GPP from 1991 to 2001 for each of the JULES scenarios and both high and low plant O_3 sensitivities against the observation-based globally extrapolated Flux Network model tree ensemble (MTE) (Jung et al., 2011). We use a paired t test to determine statistically significant differences in the mean responses.

3 Results

3.1 Impact of g_s model formulation and site-level evaluation

The impact of the g_s model on simulated g_s is shown for the site with low soil moisture stress (wet site, Fig. 2). For the broadleaf tree and C_3 herbaceous PFT, the MED model simulates a larger conductance compared to the JAC model. In other words, with the MED model these two PFTs are parameterised with a less conservative water use strategy, which, for the grid point shown in Fig. 2, increased the annual mean water use by 35 % (±29 %) and 45 % (±32 %), respectively. In contrast, the needleleaf tree, C_4 herbaceous and shrub PFTs are parameterised with a more conservative water use strategy with the MED model, and the mean annual g_s was decreased by 13 % (±12 %), 27 % (±10 %) and 36 % (±13 %), respectively, compared to the JAC model. This comparison was also performed for a dry site (high soil moisture stress), and similar results were found (Fig. S9). The effect of g_s formulation on simulated photosynthesis was much smaller because of the lower sensitivity of the limiting rates of photosynthesis to changes in c_i in the model compared to the effect of the same change in c_i on modelled g_s (Figs. S10 and S11). Changes in g_s impact the partitioning of simulated energy fluxes. In general, increased g_s results in increased latent heat and thus decreased sensible heat flux, and vice versa where g_s is decreased (Figs. S10 and S11). Also shown is the effect of the MED model on O_3 flux into the leaf (Figs. S12 and S9 bottom panel). For the broadleaf tree and C_3 herbaceous PFTs, the MED model simulates a larger conductance and therefore a greater flux of O_3 through stomata compared to JAC, and this is indicative of the potential for greater reductions in photosynthesis (Figs. S10 and S11 top row). The reverse is seen for the needleleaf tree, C_4 herbaceous and shrub PFTs.

Site-level evaluation of the seasonal cycles of latent and sensible heat with both JAC and MED models compared to FLUXNET observations showed in general the MED model improved the seasonal cycle of both fluxes (lower RMSE), but the magnitude of this varied from site to site (Fig. S13). At the deciduous broadleaf site, US-UMB, MED resulted in improvements of the simulated seasonal cycle particularly in the summer months for both fluxes (RMSE decreased from 42.7 and 31.5 to 38.5 and 28.0 $W m^{-2}$ for latent and sensible heat, respectively). At the second deciduous broadleaf site IT-CA1, however, there was almost no difference between the two g_s models. Both evergreen needleleaf forest sites (FI-Hyy and DE-Tha) saw improvements in the simulated seasonal cycles of latent and sensible heat with the MED model, primarily as a result of lower latent heat flux in the spring and summer months and higher sensible heat flux over the same period. At FI-Hyy, RMSE decreased from 10.1 and 7.4 to 6.7 and 6.7 $W m^{-2}$ for latent and sensible heat, respectively, and at DE-Tha, RMSE decreased from 16.0/11.9 to 10.5/10.6 $W m^{-2}$ for latent/sensible heat, respectively. With the MED model the monthly mean latent heat flux was improved at the C_3 grass site (CH-Cha) as a result of increased flux in the summer months (RMSE decreased from 15.7 to 13.8 $W m^{-2}$); however there was no improvement in the sensible heat flux and RMSE with MED was increased (from 3.9 to 4.9 $W m^{-2}$). At the C_4 grass site (US-SRG), small improvements were made in the seasonal cycle of both latent and sensible heat with the MED model. At the deciduous savannah site (CG-Tch), which included a high proportion of shrub PFT in the land cover type used in the site simulation, large improvements in the seasonal cycle of both fluxes were simulated with the MED model, as a result of a decrease in the latent heat flux and an increase in the sensible heat flux (RMSE decreased from 39.5 and 31.6 to 30.4 and 24.4 $W m^{-2}$ for latent and sensible heat, respectively).

3.2 Evaluation of the JULES O_3 model

For all JULES scenarios, similar spatial patterns of GPP are simulated compared to MTE (Figs. 3 and S14). MTE estimates a mean GPP for present day in Europe of 938 $gC m^2 yr^{-1}$ (Fig. 3). JULES tends to under-predict GPP relative to the MTE product. Estimates of GPP from JULES with both transient CO_2 and O_3 (run_both_CO_2+O_3) give a mean across Europe of 813 $gC m^2 yr^{-1}$ (high plant O_3 sensitivity) to 881 $gC m^2 yr^{-1}$ (low plant O_3 sensitivity), both of which are significantly different from the MTE product ($t = 27$, $d.f. = 5750$, $p < 2.2e^{-16}$ (high); $t = 4.3$, $d.f. = 5750$, $p < 1.5e^{-05}$ (low); Fig. 3). Forcing with CO_2 alone (run_CO_2) gives a mean GPP across Europe of 900 to 923 $gC m^2 yr^{-1}$ (high and low plant O_3 sensitivity, respectively), and O_3 alone (run_O_3 – without the protective effect of CO_2) reduces estimated GPP to 732 to 799 $gC m^2 yr^{-1}$ (Fig. S14). At latitudes > 45° N JULES has a tendency to under-predict MTE GPP, and at latitudes < 45° N JULES

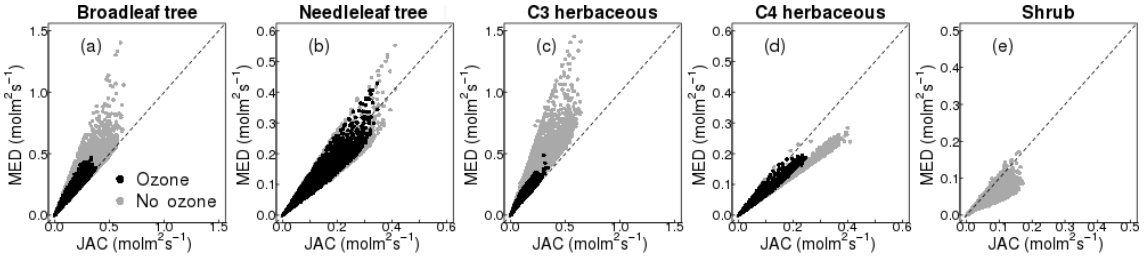

Figure 2. Comparison of simulated g_s with MED (y axis) versus JAC (x axis) for all five JULES PFTs at one grid point (lat: 48.25, long: 5.25); shown are hourly values for the year 2000.

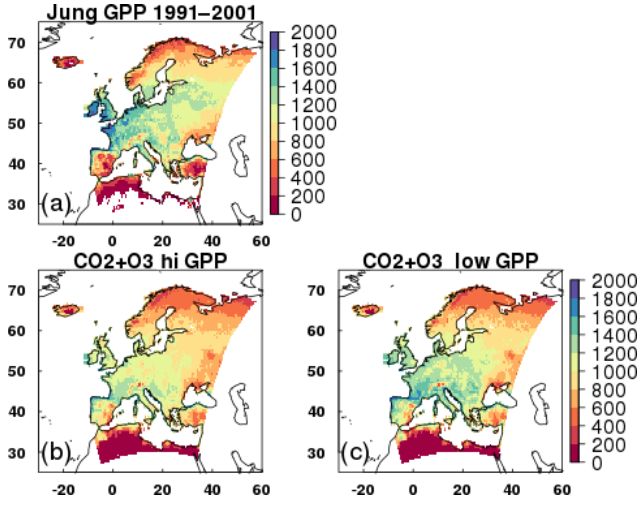

Figure 3. Mean GPP (g C m^2 yr^{-1}) from 1991 to 2001 for **(a)** the observationally based globally extrapolated Flux Network model tree ensemble (MTE) (Jung et al., 2011); **(b, c)** model simulations with transient CO_2 and transient O_3 (run_both_CO_2+O_3), with high and low plant O_3 sensitivities, respectively.

tends to over-predict MTE GPP (Fig. S15). These regional differences are highlighted in Fig. S16, in which in the Mediterranean region, JULES tends to over-predict compared to MTE GPP, so simulations with O_3 reduce the simulated GPP, bringing it closer to MTE. In the temperate region however, JULES tends to underestimate MTE GPP, so the addition of O_3 reduces simulated GPP further (Fig. S16). In the boreal region, JULES under-predicts GPP, but to a lesser extent than in the temperate region, and the addition of O_3 has less impact on reducing the GPP further (Fig. S16).

3.3 European simulations – historical period: 1901–2001

Over the historical period (1901–2001), run_O_3 reduced GPP under both the low and high plant O_3 sensitivity parameterisations by -3 to -9 %, respectively (Table 1), and this difference in simulated GPP was significant ($t = 102.2$, $d.f. = 6270$, $p < 2.2e^{-16}$). Figure 4 highlights regional variations; simulated reductions in GPP are up to 20 % across large areas of Europe, and up to 30 % in some Mediterranean regions under the high plant O_3 sensitivity. Some boreal and Mediterranean regions show small increases in GPP over this period, associated with O_3-induced stomatal closure enhancing water availability in these drier regions (Fig. 5). This allows for greater stomatal conductance later in the year when soil moisture may otherwise have been limiting to growth (up to 10 %, Fig. 5), and therefore caused higher GPP, but these regions comprise only a small area of the entire domain. Indeed, over much of Europe, O_3-induced stomatal closure led to reduced g_s (up to 20 %) across large areas of temperate Europe and the Mediterranean, and even greater reductions in some smaller regions of the southern Mediterranean (Fig. 6), and these are not associated with notable increases in soil moisture availability (Fig. 5), resulting in depressed GPP over much of Europe as described above. Under the low plant O_3 sensitivity, similar spatial patterns occur, but the magnitude of GPP change (up to -10 % across much of Europe) and g_s change (-5 to -10 %) is lower compared to the high sensitivity. Over the twentieth century the land carbon sink is suppressed (-2 to -6 %, Table 1). Large regional variation is shown in Fig. 4, with temperate and Mediterranean Europe seeing a large reduction in land carbon storage, particularly under the high plant O_3 sensitivity (up to -15 %).

Combined, the physiological response to changing CO_2 and O_3 concentrations (run_both_CO_2+O_3) results in a net loss of land carbon over the twentieth century under the high plant O_3 sensitivity (-2 %, Table 1), dominated by loss of soil carbon (Table S3). This reflects the large increases in tropospheric O_3 concentration observed over this period (Fig. 1). Under low plant O_3 sensitivity, the land carbon sink has started to recover by 2001 (+1.5 %) owing to the recovery of the soil carbon pool beyond 1901 values over this period (Table S3).

To gain perspective on the magnitude of the O_3-induced flux of carbon from the land to the atmosphere we relate changes in total land carbon to carbon emissions from fossil fuel combustion and cement production for the EU28-plus countries (EU-28 plus Albania, Bosnia and Herzegovina, Iceland, Belarus, Serbia, Moldova, Norway, Turkey, Ukraine, Switzerland and Macedonia) from the data of Boden et al. (2013). We recognise that our simulation domain is

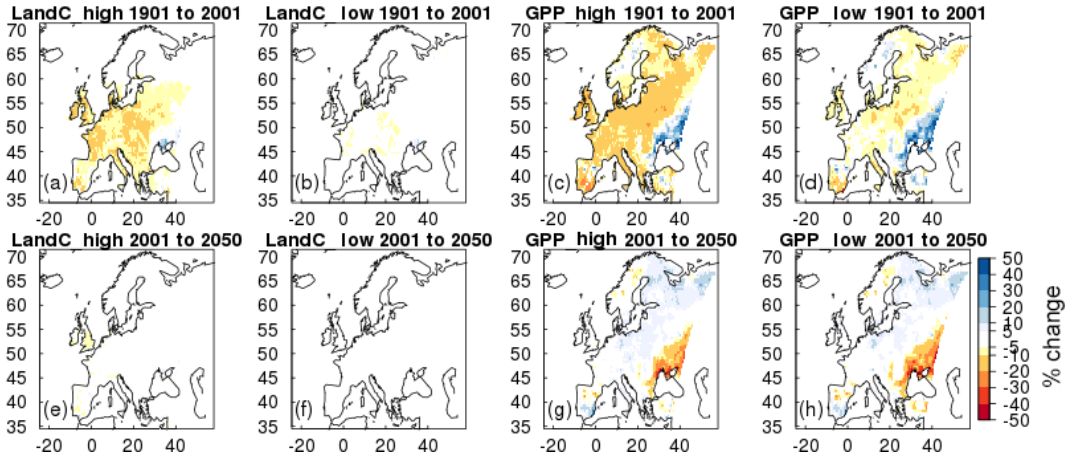

Figure 4. Simulated percentage change in total carbon stocks (Land C) and gross primary productivity (GPP) due to O_3 effects at fixed pre-industrial atmospheric CO_2 concentration (run_O_3). Changes are shown for the periods 1901 to 2001 and 2001 to 2050 for the high and low plant O_3 sensitivities.

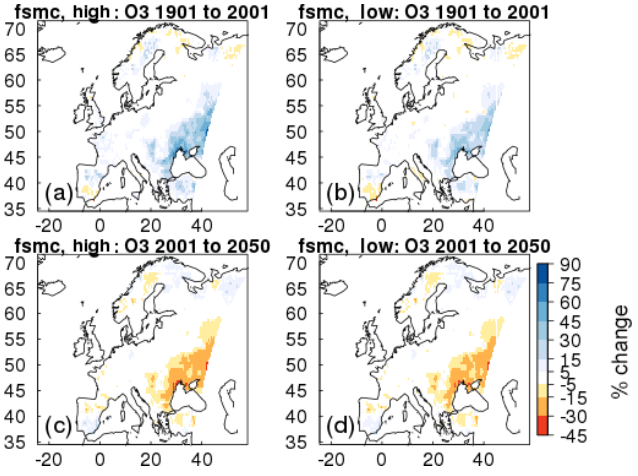

Figure 5. Simulated percentage change in plant available soil moisture (fsmc) due to O_3 effects at fixed pre-industrial atmospheric CO_2 concentration (run_O_3). Changes are shown for the periods 1901 to 2001 and 2001 to 2050 for the high and low plant O_3 sensitivities.

slightly larger than the EU28-plus as it includes a small area of western Russia so direct comparisons cannot be made, but this still provides a useful measure of the size of the carbon flux. For the period 1970 to 1979 the simulated loss of carbon from the European terrestrial biosphere due to O_3 effects on vegetation physiology was on average 1.32 Pg C (high vegetation sensitivity) and 0.71 Pg C (low vegetation sensitivity) (Table 2). This O_3-induced reduced C uptake of the land surface is equivalent to around 8 to 16 % of the emissions of carbon from fossil fuel combustion and cement production over the same period for the EU28-plus countries (Table 2). Currently the emissions data availability goes up to 2011. Over the last observable decade (2002 to 2011) the simulated reduction in land carbon due to O_3 has declined, but is still equivalent to 2 to 4 % of the emissions of carbon from fossil fuels and cement production for the EU28-plus countries (Table 2). By comparison with one of the largest anthropogenic emissions of carbon for Europe, we show here that the potential effect of O_3 on reducing the size of the European land carbon sink is notable.

3.4 European simulations – future period: 2001–2050

Over the 2001 to 2050 period, region-wide GPP with O_3 only changing (run_O_3) increased marginally (+0.1 to +0.2 %, high and low plant O_3 sensitivities; Table 1, with a significant difference between the two plant O_3 sensitivities; $t = 57$, $d.f. = 6270$ $p < 2.2e^{-16}$), although with large spatial variability as discussed below (Fig. 4g and h). Figures S7 and S8 show that despite decreased tropospheric O_3 concentrations by 2050 in summer compared to 2001 levels, all regions are exposed to an increase in O_3 over the wintertime, and some regions of Europe, particularly temperate and Mediterranean regions experience increases in O_3 concentration in spring and autumn. Therefore, although in the O_3 simulation overall simulated GPP for Europe shows a small increase, large spatial variability is shown in Fig. 4g and h because of the variability in O_3 concentration with region and season. Increased GPP (dominantly 10, but up to 20 % in some areas) on 2001 levels is simulated across areas of Europe; however, decreases of up to 21 % are simulated in some areas of the Mediterranean, up to 15 % in some areas of the boreal region and up to 27 % in the temperate zone (Fig. 4g and h).

When O_3 and CO_2 effects are combined (run_both_CO_2+O_3), simulated GPP increases (+15 to +18 %, high and low plant O_3 sensitivities, respectively, Table 1). This increase is greater than the enhancement simulated when CO_2 affects plant growth independently

Table 1. Simulated changes in the European land carbon cycle due to changing O_3 and CO_2 concentrations (independently and together). Shown are changes in total carbon stocks (Land C) and gross primary productivity (GPP) over three different periods (historical: 1901 to 2001; future: 2001 to 2050; and full time series: 1901 to 2050). Absolute (top) and relative (bottom) differences are shown. For 2001 to 2050, please refer to Table S4 for the initial value for each run. See the Supplement for details of the estimation of the O_3 and CO_2 effects and their interaction.

	High plant O_3 sensitivity					
	1901–2001		2001–2050		1901–2050	
	GPP ($Pg\,C\,yr^{-1}$)	Land C ($Pg\,C$)	GPP ($Pg\,C\,yr^{-1}$)	Land C ($Pg\,C$)	GPP ($Pg\,C\,yr^{-1}$)	Land C ($Pg\,C$)
Value in 1901	9.05	167	–	–	9.05	167
Absolute change						
O_3	−0.81	−9.21	0.01	−2.44	−0.80	−11.65
CO_2	1.16	4.24	1.42	12.98	2.58	17.22
$CO_2 + O_3$	0.13	−3.28	1.66	11.11	1.79	7.83
% change						
O_3	−8.95	−5.51	0.12	−1.55	−8.84	−6.98
CO_2	12.82	2.54	13.91	7.58	28.51	10.31
$CO_2 + O_3$	1.44	−1.96	18.08	6.79	19.78	4.69
	Low plant O_3 sensitivity					
	1901–2001		2001–2050		1901–2050	
	GPP ($Pg\,C\,yr^{-1}$)	Land C ($Pg\,C$)	GPP ($Pg\,C\,yr^{-1}$)	Land C ($Pg\,C$)	GPP ($Pg\,C\,yr^{-1}$)	Land C ($Pg\,C$)
Value in 1901	9.34	167.5	–	–	9.34	167.5
Absolute change						
O_3	−0.30	−3.59	0.02	−1.07	−0.40	−4.66
CO_2	1.15	6.43	1.35	13.14	2.50	19.57
$CO_2 + O_3$	0.65	2.50	1.50	12.35	2.15	14.85
% change						
O_3	−3.21	−2.14	0.22	−0.65	−4.28	−2.78
CO_2	12.31	3.84	12.87	7.55	26.77	11.68
$CO_2 + O_3$	6.96	1.49	15.02	7.26	23.02	8.87

(run_CO_2) because additional O_3-induced stomatal closure increases soil water availability in some regions, which enhances growth more in run_both_CO_2+O_3, compared to run_CO_2. Nevertheless, although the percentage gain is larger, the absolute value of GPP by 2050 remains lower in run_both_CO_2+O_3 compared to GPP in run_CO_2, highlighting the negative impact of O_3 at the land surface (Table S4).

Despite small increases in GPP in run_O_3, the land carbon sink continues to decline from 2001 levels (−0.7 to −1.6 %, low and high plant O_3 sensitivities, respectively; Table 1). This is because the soil and vegetation carbon pools continue to lose carbon as they adjust slowly to small changes in input (GPP); i.e. the soil carbon pool is not in equilibrium in 2001, and is declining in response to reduced litter input as a result of twentieth century O_3 impacts on GPP. Nevertheless, the negative effect of O_3 on the future land sink is markedly reduced relative to the historical period. Figure 4e and f, however, highlight regional differences. Boreal regions and parts of central Europe see minimal O_3 damage, whereas some areas of southern and northern Europe see further losses of up to 8 % on 2001 levels. The run_both_CO_2+O_3 simulation is dominated by the physiological effects of changing CO_2, with land carbon sink increases of up to 7 % (Table 1).

3.5 European simulations – full experimental period: 1901–2050

From 1901 to 2050, run_O_3 reduces GPP (−4 to −9 %, with a significant difference between the low and high plant O_3 sensitivities ($t = 95, d.f. = 6270\ p < 2.2e^{-16}$)) and land car-

Table 2. Simulated change in total land carbon due to O_3 damage with changing atmospheric CO_2 concentration for the two vegetation sensitivities. The sum of carbon emissions for each decade from fossil fuel combustion and cement production for the EU28 plus Albania, Bosnia and Herzegovina, Iceland, Belarus, Serbia, Moldova, Norway, Turkey, Ukraine, Switzerland and Macedonia (EU28-plus) is shown; the data are from Boden et al. (2013). The simulated change in land carbon as a result of O_3 damage is depicted as a percentage of the EU28-plus emissions to demonstrate the magnitude of the additional source of carbon to the atmosphere from plant O_3 damage.

	Mean (Pg C)				
	1970–1979	1980–1989	1990–1999	2000–2009	2002–2011
Modelled O_3 effect on land C sink					
Higher sensitivity	−1.32	−1.01	−0.97	−0.53	−0.50
Low sensitivity	−0.71	−0.58	−0.50	−0.29	−0.26
Sum of C emissions from fossil fuel combustion and cement production (Pg C)	8.39	8.63	12.26	12.83	12.75
C lost from O_3 effect as a percentage of fossil fuel and cement emissions (%)					
Higher sensitivity	−15.73	−11.70	−7.91	−4.13	−3.92
Low sensitivity	−8.46	−6.72	−4.08	−2.26	−2.04

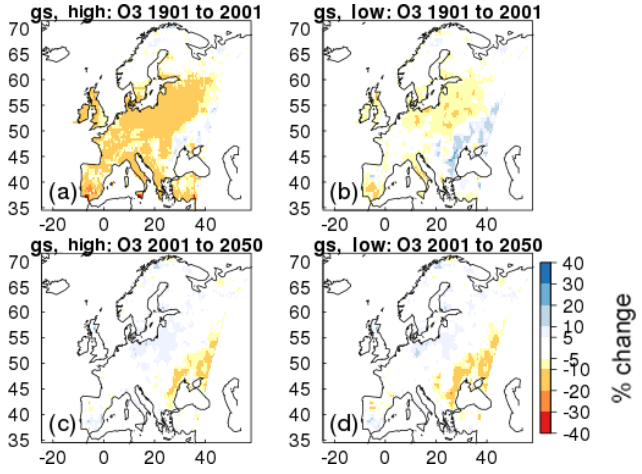

Figure 6. Simulated percentage change in stomatal conductance (g_s) due to O_3 effects at the fixed pre-industrial atmospheric CO_2 concentration (run_O_3). Changes are shown for the periods 1901 to 2001 and 2001 to 2050 for the high and low plant O_3 sensitivities.

bon storage (−3 to −7 %, Table 1). Regionally, O_3 damage is lowest in the boreal zone. GPP decreases are largely between 5–8% and 2–4 % for the high and low plant O_3 sensitivities, respectively, with large areas minimally affected by O_3 damage (Fig. 7), consistent with lower g_s values of needleleaf trees that dominate this region, and so lower O_3 uptake (Figs. S17 and S18). In the temperate region, O_3 damage is extensive, with reductions in GPP dominantly from 10 to 15 % for the low and high plant O_3 sensitivities, respectively. Across significant areas of this region reductions in GPP are up to 20 % under high plant O_3 sensitivity (Fig. 7). In the Mediterranean region, O_3 damage reduces GPP by 5 to 15 % and 3 to 6 % for the high and low plant O_3 sensitivities, respectively, with some areas seeing greater losses of up to 20 % under the high plant O_3 sensitivity, but this is less extensive than that seen in the temperate zone (Fig. 7). In these drier regions, O_3-induced stomatal closure can increase available soil moisture (Fig. S17 and S18).

The run_both_CO_2+O_3 simulation shows that CO_2-induced stomatal closure can help alleviate O_3 damage by reducing the uptake of O_3 (Table S6). In these simulations, CO_2-induced stomatal closure was found to offset O_3 suppression of GPP, such that GPP by 2050 is 3 to 7 % lower due to O_3 exposure (run_both_CO_2+O_3), rather than 4 to 9 % lower in the absence of increasing CO_2 (run_O_3, Table S6). Figure 6 shows this spatially, O_3 damage is reduced when the effect of atmospheric CO_2 on stomatal closure is accounted for; however, despite this, the land carbon sink and GPP remain significantly reduced due to O_3 exposure.

From 1901 to 2050, run_both_CO_2+O_3 results in an increase in European land carbon uptake (+5 to +9 %) and an increase in GPP (+20 to +23 %) by 2050 for the high and low plant O_3 sensitivities, respectively (Table 1). Nevertheless, despite this increase there remains a large negative impact of O_3 on the European land carbon sink (Fig. S19). By 2050 the simulated enhancement of land carbon and GPP in response to elevated CO_2 alone (run_CO_2) is reduced by 3 to 6 % (land carbon) and 4 to 9 % (GPP) for the low and high plant O_3 sensitivities, respectively, when O_3 is also accounted for (run_both_CO_2+O_3, Table 1). This is a large reduction in the ability of the European terrestrial biosphere to sequester carbon.

4 Discussion

4.1 Evaluation of g_s models and JULES O_3 model

Comparison of the new g_s model implemented in this study (MED) with the g_s model currently used as a standard in JULES (JAC) revealed large differences in g_s for each PFT, principally as a result of the data-based parameterisation of the new model. Water use increased for the broadleaf tree and C_3 herbaceous PFTs using the MED model compared to JAC, but decreased for the needleleaf tree, C_4 herbaceous and shrub PFTs, which displayed a more conservative water use strategy compared to JAC. These changes are in line with the work of De Kauwe et al. (2015), who found a reduction in annual transpiration for evergreen needleleaf, tundra and C_4 grass regions when implementing the Medlyn g_s model into the Australian land surface scheme CABLE. Site-level evaluation of the models against FLUXNET observations showed that in general the MED model improved simulated seasonal cycles of latent and sensible heat. The magnitude of the improvement varied with site; improvements were seen at the deciduous savanna site, and at the needleleaf tree sites and broadleaf tree site (US_UMB) in the spring and summer. However, much smaller improvements were seen at the grass sites. Changes in g_s in this study resulted in differences in latent and sensible heat fluxes. Changes in the partitioning of energy fluxes at the land surface could have consequences for the intensity of heatwaves (Cruz et al., 2010; Kala et al., 2016), run-off (Betts et al., 2007; Gedney et al., 2006) and rainfall patterns (de Arellano et al., 2012), although fully coupled simulations would be necessary to detect these effects. The differences in simulated g_s led to differences in uptake of O_3 between the two models because the rate of g_s is the predominant determinant of the flux of O_3 through stomata. Higher O_3 uptake is indicative of greater damage. Therefore, given that C_3 herbaceous vegetation is the dominant land cover class across the European domain used in this study, this suggests a greater O_3 impact for Europe would be simulated with the MED model compared to JAC in our simulations in which chemistry is uncoupled from the land surface.

We evaluated the JULES O_3 model by comparing modelled GPP against the Jung et al. (2011) MTE product. Similar spatial patterns of GPP were simulated by JULES compared to MTE. Zonal means also showed similar patterns of GPP, although JULES under-predicted GPP compared to MTE at latitudes $>45°$ N (temperate and boreal regions; all simulations) and over-predicted GPP at latitudes $<45°$ N (Mediterranean region; all simulations). The simulations with transient O_3 (i.e. O_3 and CO_2+O_3) showed large differences in GPP between the high and low plant O_3 sensitivity simulations, which is to be expected given that the high plant O_3 sensitivity simulations were parameterised to be "damaged" more by O_3, i.e. greater reduction of photosynthesis and g_s with O_3 exposure compared to the low plant O_3 sensitivity simulations. This difference was largest in the temperate zone, largely because of C_3 grass cover being the dominant land cover here and the difference in the sensitivity to O_3 between the high and low calibrations is significantly larger for C_3 grasses compared to the needleleaf trees that dominate in the boreal region. Additionally, a longer growing season in the temperate region may allow for greater uptake of O_3 into vegetation. C_3 grass is also the dominant land cover in the Mediterranean region with a different calibration used for Mediterranean grasses for the low plant O_3 sensitivity, which is less sensitive to O_3 than the temperate C_3 grasses, but high soil moisture stress is common throughout the growing season in the Mediterranean, limiting the uptake of O_3 through stomata, which likely diminishes the difference between the high and low calibrations. In general, incorporating plant O_3 damage into JULES leads to worse agreement with the MTE GPP product; however, this is expected to some degree as we are adding an explicit representation of O_3 damage to a model calibrated to reproduce present-day GPP and drawdown of atmospheric CO_2. Inevitably this implicitly includes O_3 damage to vegetation. Explicit representation of plant O_3 damage is important to investigate how O_3 damage changes through time under different emissions scenarios and the interactive effects with other gases (such as CO_2) and with climate change. The percentage changes we simulate are therefore important to demonstrate the sensitivity of modelled GPP and land carbon to this process.

4.2 Comparison of modelled estimates of O_3 damage

Our estimates suggest O_3 (run_O_3) reduced GPP by 2001 by 3 to 9 % on average across Europe and NPP by 5 to 11 % for the low and high plant O_3 sensitivities, respectively (Table S3). Anav et al. (2011) simulated a 22 % reduction of GPP across Europe for 2002 using the ORCHIDEE model. Present-day O_3 exposure reduced GPP by 10 to 25 % in Europe and 10.8 % globally in the study by Lombardozzi et al. (2015) using the Community Land Model (CLM). O_3 reduced NPP by 11.2 % in Europe from 1989 to 1995 using the Terrestrial Ecosystem Model (TEM) (Felzer et al., 2005). Globally, concentrations of O_3 predicted for 2100 reduced GPP by 14 to 23 % using a former parameterisation of O_3 sensitivity in JULES (Sitch et al., 2007). The recent study by Franz et al. (2017) showed mean GPP declined by 4.7 % over the period 2001 to 2010 using the OCN model over the same European domain and using the same O_3 forcing produced by EMEP MSC-W as used in this study. Our estimates of changes in present-day GPP and NPP are at the lower end of previously modelled estimates. Simulated O_3 impacts will be dependent on model O_3 concentrations, meteorology, plant sensitivity to O_3 and process representation of O_3 damage. It is therefore difficult to hypothesise exactly why modelled estimates differ, but it is suggested that an ensemble approach to modelling O_3 impacts on the terrestrial biosphere would be

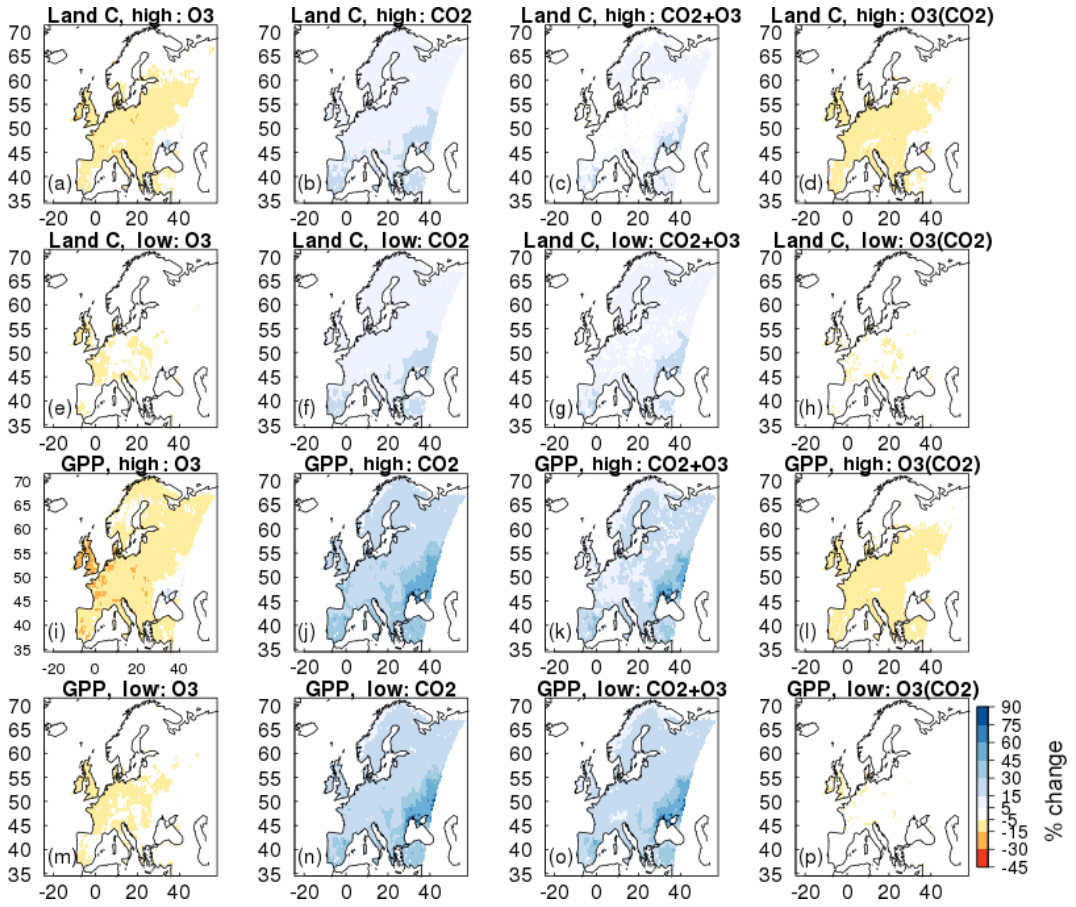

Figure 7. Simulated percentage change in total carbon stocks (Land C) and gross primary productivity (GPP) due to (i) **(a, e, i, m)** O_3 effects at fixed pre-industrial atmospheric CO_2 concentration (run_O_3), (ii) **(b, f, j, n)** CO_2 fertilisation at fixed pre-industrial O_3 concentration (run_CO_2), (iii) **(c, g, k, o)** the interaction between O_3 and CO_2 effects (run_both_CO_2+O_3), and (iv) **(d, h, l, p)** O_3 effects with changing atmospheric CO_2 concentration (i.e. O_3 damage accounting for the effect of CO_2-induced stomatal closure; run_both_CO_2+O_3 – run_CO_2). Changes are depicted for the period from 1901 to 2050 for high and low ozone plant sensitivities.

beneficial to understand some of these differences and provide estimates of O_3 damage with uncertainties.

4.3 Impacts of O_3 at the land surface

In this study, O_3 has a detrimental effect on the size of the land carbon sink for Europe. This is primarily through a decrease in the size of the soil carbon pool as a result of reduced litter input to the soil, consistent with reduced GPP and NPP. Field studies show that in some regions of Europe, soil carbon stocks are decreasing (Bellamy et al., 2005; Capriel, 2013; Heikkinen et al., 2013; Sleutel et al., 2003). The study of Bellamy et al. (2005), for example, showed that carbon was lost from soils across England and Wales between 1978 and 2003 at a mean rate of 0.6 % per year with little effect of land use on the rate of carbon loss, suggesting a possible link to climate change. It is understood that climate change is likely to affect soil carbon turnover. Increased temperatures increase microbial decomposition activity in the soil and therefore increase carbon losses through higher rates of respiration (Cox et al., 2000; Friedlingstein et al., 2006; Jones et al., 2003). However, some studies have found that O_3 can decrease soil carbon content. Talhelm et al. (2014), for example, found O_3 reduced carbon content in near surface mineral soil of forest soils exposed to 11 years of O_3 fumigation. Hofmockel et al. (2011) found elevated O_3 reduced the carbon content in more stable soil organic matter pools, and Loya et al. (2003) showed that the fraction of soil carbon formed in forest soils over a 4-year experimental period when fumigated with both CO_2 and O_3 was reduced by 51 % compared to the soil fumigated with CO_2 alone. It is agreed that amongst other factors that change with O_3 exposure such as litter quality and composition, reduced litter quantity also has significant detrimental consequences for soil carbon stocks (Andersen, 2003; Lindroth, 2010; Loya et al., 2003). Results from this study therefore suggest that increasing tropospheric O_3 may be a contributing factor to the declining soil carbon stocks observed across Europe as a result of reduced litter input to the soil carbon pool consistent with reduced NPP.

We acknowledge, however, that our model simulations do not include coupling of nitrogen and carbon cycles or land management practices. We include a representation of agricultural regions through the model calibration against the wheat O_3 sensitivity function (CLRTAP, 2017), and in our simulations the high plant O_3 sensitivity scenario uses this calibration against wheat for all C_3/C_4 land cover, which dominates our model domain. Wheat is known to be one of the most O_3-sensitive crop species, however, so it is possible that our simulations overestimate the O_3 impact at the land surface. However, the low plant O_3 sensitivity calibration against natural grasslands provides a counter estimate of the impact of O_3 at the land surface; therefore it is important to consider the range our results provide (i.e. both the high and low plant O_3 sensitivities) as an indicator of the impact of O_3 on the land surface. As with all uncoupled modelling studies, a change in g_s and flux will impact the O_3 concentration itself. Therefore adopting the Medlyn formulation with a higher g_s values and subsequently higher O_3 flux for broadleaf and C_3 PFTs (Fig. 2) would lead to reduced O_3 concentration, which in turn may dampen the effect of higher g_s on O_3 flux. Although the higher uptake of O_3 by vegetation may lead to more damage and increase O_3 concentrations, in an uncoupled chemistry–land modelling system such as this it is not possible to predict which process would dominate. Additionally, this version of JULES does not have a crop module; it has no land management practices such as harvesting, ploughing or crop rotation – processes which may have counteracting effects on the land carbon sink. Further, without a coupled carbon and nitrogen cycle, it is likely that the CO_2 fertilisation response of GPP and the land carbon sink is overestimated in some regions of our simulations since nitrogen availability limits terrestrial carbon sequestration of natural ecosystems in the temperate and boreal zone (Zaehle, 2013). This would have consequences for our modelled O_3 impact, particularly into the future when the large CO_2 fertilisation effect was responsible for partly offsetting the negative impact of O_3. However, in our simulations a high fraction of land cover is agricultural, which we assume would be optimally fertilised. Our simulations also use a fixed climate, so we do not include the effect of climate change on shifting plant phenology. Therefore, our results may underestimate plant O_3 damage since if the growing season started earlier or finished later plants in some regions would be exposed to higher O_3 concentrations. Nevertheless, we emphasise that this study provides a sensitivity assessment of the impact of plant O_3 damage on GPP and the land carbon sink.

Another caveat we fully acknowledge is that at the leaf level JULES is parameterised to reduce g_s with O_3 exposure. Whilst this response is commonly observed (Wittig et al., 2007; Ainsworth et al., 2012), there is evidence to suggest that O_3 impairs stomata in some species, making them non-responsive to environmental stimuli (Hayes et al., 2012; Hoshika et al., 2012a; Mills et al., 2009; Paoletti and Grulke, 2010). In drought conditions the mechanism is thought to involve O_3-stimulated ethylene production, which interferes with the stomatal response to abscisic acid (ABA) signalling (Wilkinson and Davies, 2009, 2010). Such stomatal sluggishness can result in higher O_3 uptake and injury, increased water loss, and therefore greater vulnerability to environmental stresses (Mills et al., 2016). McLaughlin (2007a, b) and Sun et al. (2012) provide evidence of increased transpiration and reduced streamflow in forests at the regional scale in response to ambient levels of O_3 and suggest this could increase the frequency and severity of droughts. Hoshika et al. (2012b), however found that despite sluggish stomatal control in O_3-exposed trees, whole tree water use was lower in these trees because of lower gas exchange and premature leaf shedding of injured leaves. To our knowledge, the study of Hoshika et al. (2015) is the first to include an explicit representation of sluggish stomatal control in a land–atmosphere model. They show that sluggish stomatal behaviour has implications for carbon and water cycling in ecosystems. However, it is by no means a ubiquitous response, and it is not fully understood which species respond this way and under what conditions (Mills et al., 2016; Wittig et al., 2007). Nevertheless, this remains an important area of future work.

In this work we implement the stomatal closure proposed in Medlyn et al. (2011), which uses the parameter g_1. Hoshika et al. (2013) show a significant difference in the g_1 parameter (higher in elevated O_3 compared to ambient) in Siebold's beech in June of their experiment. However, this is only at the start of the growing season; further measurements show no difference in this parameter among O_3 treatments. Quantifying an O_3 effect directly on g_1 would require a detailed meta-analysis of empirical data on photosynthesis and g_s for different PFTs, which is currently lacking in the literature.

A further caveat of this study is that the O_3 concentrations used to force the model are offline, in this case generated by the EMEP MSC-W model. This means the depositional sink is different in JULES (Medlyn formulation) compared to the EMEP model, which uses the g_s formulation presented in Emberson et al. (2000, 2001). Because we link two different model systems, the g_s values in the EMEP model differ from those obtained using the Medlyn formulation, which would ultimately lead to different O_3 concentrations. The role of EMEP in this study is to provide O_3 concentrations at the top of the vegetation canopy to force JULES and not g_s; how the different depositional sinks would affect simulated O_3 concentrations at canopy height has not been investigated.

These offline simulations show the sensitivity of GPP and the land carbon sink to tropospheric O_3, suggesting that O_3 is an important predictor of future GPP and the land carbon store across Europe. There are uncertainties in our estimates, however, from the use of uncoupled tropospheric chemistry, meteorology and stomatal function. For example, increased frequency of drought in the future would reduce stomatal conductance (assuming no sluggish stomatal response) and thus O_3 uptake. Since our offline simulations do not include

this feedback, it is possible the O_3 effect is overestimated here. Given the complexity of potential interactions and feedbacks, it remains difficult to diagnose the importance of individual factors (e.g. the direct physiological response) in a fully coupled simulation. Once the importance of a process is demonstrated offline, it provides evidence of the need to incorporate such a process in coupled regional and global simulations.

4.4 O_3 as a missing component of carbon cycle assessments?

Comprehensive analyses of the European carbon balance suggest a large biogenic carbon sink (Janssens et al., 2003; Luyssaert et al., 2012; Schulze et al., 2009). However, estimates are hampered by large uncertainties in key components of the land carbon balance, such as estimates of soil carbon gains and losses (Ciais et al., 2010; Janssens et al., 2003; Schulze et al., 2009, 2010). We suggest that the effect of O_3 on plant physiology is a contributing factor to the decline in soil carbon stores observed across Europe, and as such this O_3 effect is a missing component of European carbon cycle assessments. Over the full experimental period (1901 to 2050), our results show elevated O_3 concentrations reduce the amount of carbon that can be stored in the soil by 3 to 9 % (low and high plant O_3 sensitivities, respectively), which almost completely offsets the beneficial effects of CO_2 fertilisation on soil carbon storage under the high plant O_3 sensitivity . This would contribute to a change in the size of a key carbon sink for Europe and is particularly important when we consider the evolution of the land carbon sink into the future given the impact of O_3 on soil carbon sequestration and the high uncertainty of future tropospheric O_3 concentrations. Schulze et al. (2009) and Luyssaert et al. (2012) extended their analysis of the European carbon balance to include additional non-CO_2 greenhouse gases (CH_4 and N_2O). Both studies found that emissions of these offset the biogenic carbon sink, reducing the climate mitigation potential of European ecosystems. This highlights the importance of accounting for all fluxes and stores in carbon and greenhouse gas balance assessments, of which O_3 and its indirect effect on the CO_2 flux via direct effects on plant physiology are currently missing.

4.5 Interactive effects of O_3 and CO_2

We looked at the interactive effects of CO_2 and O_3. Our results support the hypothesis that elevated atmospheric CO_2 provides some protection against O_3 damage because of lower g_s that reduces uptake of O_3 through stomata (Harmens et al., 2007; Wittig et al., 2007). In the present study, reductions in GPP and the land carbon store due to O_3 exposure were lower when simulated with concurrent changes in atmospheric CO_2. Despite acclimation of photosynthesis after long-term exposure to elevated atmospheric CO_2 of field-grown plants (Ainsworth and Long, 2005; Medlyn et al., 1999), there is no evidence to suggest that g_s acclimates (Ainsworth et al., 2003; Medlyn et al., 2001). This suggests the protective effect of elevated atmospheric CO_2 against O_3 damage will be sustained in the long term. However, although meta-analysis suggests a general trend of reduced g_s with elevated CO_2 (Ainsworth and Long, 2005; Medlyn et al., 1999), this is not a universal response. Stomatal responses to exposure to elevated CO_2 with FACE treatment varied with genotype and growth stage in a fast-growing poplar community (Bernacchi et al., 2003; Tricker et al., 2009). In other mature forest stands, limited stomatal response to elevated CO_2 was observed after canopy closure (Ellsworth, 1999; Uddling et al., 2009). Also, some studies found that stomatal responses to CO_2 were significant only under high atmospheric humidity (Cech et al., 2003; Leuzinger and Körner, 2007; Wullschleger et al., 2002). These examples illustrate that stomatal responses to elevated atmospheric CO_2 are not universal, and as such the protective effect of CO_2 against O_3 injury cannot be assumed for all species at all growth stages under wide-ranging environmental conditions.

5 Conclusions

What is abundantly clear is that plant responses to both CO_2 and O_3 are complicated by a host of factors that are only partly understood, and it remains difficult to identify general global patterns given that effects of both gases on plant communities and ecological interactions are highly context and species specific (Ainsworth and Long, 2005; Fuhrer et al., 2016; Matyssek et al., 2010b). This study quantifies the sensitivity of the land carbon sink for Europe and GPP to changing concentrations of atmospheric CO_2 and O_3 from 1901 to 2050. We have used a state-of-the-art land surface model calibrated for European vegetation to give our best estimates of this sensitivity within the limits of data availability to calibrate the model for O_3 sensitivity, current knowledge and model structure. In summary, this study has shown that potential gains in terrestrial carbon sequestration over Europe resulting from elevated CO_2 can be partially offset by concurrent rises in tropospheric O_3 over 1901–2050. Specifically, we have shown that the negative effect of O_3 on the land carbon sink was greatest over the twentieth century, when O_3 concentrations increased rapidly from pre-industrial levels. Over this period soil carbon stocks were diminished over agricultural areas, consistent with reduced NPP and litter input. This loss of soil carbon was largely responsible for the decrease in the size of the land carbon sink over Europe. The O_3 effect on the land carbon store and flux was reduced into the future as CO_2 concentration rose considerably and changes in O_3 concentration were less pronounced. However, there remained a large cumulative negative impact on the land carbon sink for Europe by 2050. The interaction between the two gases was found to reduce O_3

injury owing to reduced stomatal opening in elevated atmospheric CO_2. However, primary productivity and land carbon storage remained suppressed by 2050 due to plant O_3 damage. Expressed as a percentage of the emissions from fossil fuel and cement production for the EU28-plus countries, the carbon emissions from O_3-induced plant injury are a source of anthropogenic carbon previously not accounted for in carbon cycle assessments. Our results demonstrate the sensitivity of modelled terrestrial carbon dynamics to the direct effect of tropospheric O_3 and its interaction with atmospheric CO_2 on plant physiology, demonstrating this process is an important predictor of future GPP and trends in the land carbon sink. Nevertheless, this process remains largely unconsidered in regional and global climate model simulations that are used to model carbon sources and sinks and carbon–climate feedbacks.

Data availability. The JULES model can be downloaded from the Met Office Science Repository Service (https://code.metoffice.gov.uk/trac/jules, last access: 11 September 2017 – see here for a helpful how-to http://jules.jchmr.org/content/getting-started, last access: 11 September 2017). Model output data presented in this paper and the exact version of JULES with name lists are available upon request from the corresponding author.

The Supplement related to this article is available online at https://doi.org/10.5194/bg-15-4245-2018-supplement.

Author contributions. RJO performed the JULES model simulations and analysis. DS provided regional tropospheric ozone forcing from the EMEP MSC-W model. All authors wrote the paper.

Competing interests. The authors declare that they have no conflict of interest.

Acknowledgements. Rebecca J. Oliver and Lina M. Mercado were supported by the EU FP7 (ECLAIRE, 282910) and JWCRP (UKESM, NEC05816). This work was also supported by EMEP under UNECE. Stephen Sitch and Lina M. Mercado acknowledge the support of the NERC SAMBBA project (NE/J010057/1). The UK Met Office contribution was funded by BEIS under the Hadley Centre Climate Programme (GA01101). Gerd A. Folberth also acknowledges funding from the EU's Horizon 2020 research and innovation programme (CRESCENDO, 641816). We also thank Magnuz Engardt of SMHI for providing the RCA3 climate dataset. This work used eddy covariance data acquired and shared by the FLUXNET community, including these networks: AmeriFlux, AfriFlux, AsiaFlux, CarboAfrica, CarboEuropeIP, CarboItaly, CARBOMONT, ChinaFLUX, FLUXNET Canada, GreenGrass, ICOS, KoFlux, LBA, NECC, TERN OzFlux, TCOS Siberia and USCCC. The ERA-Interim reanalysis data are provided by ECMWF and processed by LSCE. The FLUXNET eddy covariance data processing and harmonisation was carried out by the European Fluxes Database Cluster, AmeriFlux Management Project and Fluxdata project of FLUXNET, with the support of CDIAC and the ICOS Ecosystem Thematic Centre and the OzFlux, ChinaFlux, and AsiaFlux offices. We also thank the two anonymous reviewers, who helped to improve this paper.

Edited by: Xinming Wang
Reviewed by: two anonymous referees

References

Ainsworth, E. and Long, S.: What have we learned from 15 years of free-air CO_2 enrichment (FACE)? A meta-analytic review of the responses of photosynthesis, canopy properties and plant production to rising CO_2, New Phytol., 165, 351–372, 2005.

Ainsworth, E. A., Davey, P. A., Hymus, G. J., Osborne, C. P., Rogers, A., Blum, H., Nosberger, J., and Long, S. P.: Is stimulation of leaf photosynthesis by elevated carbon dioxide concentration maintained in the long term? A test with *Lolium perenne* grown for 10 years at two nitrogen fertilization levels under Free Air CO_2 Enrichment (FACE), Plant, Cell Environ., 26, 705–714, 2003.

Ainsworth, E. A.: Rice production in a changing climate: a meta-analysis of responses to elevated carbon dioxide and elevated ozone concentration, Glob. Change Biol., 14, 1642–1650, https://doi.org/10.1111/j.1365-2486.2008.01594.x, 2008.

Ainsworth, E. A., Yendrek, C. R., Sitch, S., Collins, W. J., and Emberson, L. D.: The Effects of Tropospheric Ozone on Net Primary Productivity and Implications for Climate Change, Annu. Rev. Plant Biol., 63, 637–661, https://doi.org/10.1146/annurev-arplant-042110-103829, 2012.

Anav, A., Menut, L., Khvorostyanov, D., and Viovy, N.: Impact of tropospheric ozone on the Euro-Mediterranean vegetation, Glob. Change Biol., 17, 2342–2359, 2011.

Andersen, C. P.: Source–sink balance and carbon allocation below ground in plants exposed to ozone, New Phytol., 157, 213–228, https://doi.org/10.1046/j.1469-8137.2003.00674.x, 2003.

Arneth, A., Harrison, S. P., Zaehle, S., Tsigaridis, K., Menon, S., Bartlein, P. J., Feichter, J., Korhola, A., Kulmala, M., O'Donnell, D., Schurgers, G., Sorvari, S., and Vesala, T.: Terrestrial biogeochemical feedbacks in the climate system, Nat. Geosci., 3, 525–532, 2010.

Auvray, M. and Bey, I.: Long-range transport to Europe: Seasonal variations and implications for the European ozone budget, J. Geophys. Res.-Atmos., 110, D11303, https://doi.org/10.1029/2004JD005503, 2005.

Avnery, S., Mauzerall, D. L., Liu, J., and Horowitz, L. W.: Global crop yield reductions due to surface ozone exposure: 1. Year 2000 crop production losses and economic damage, Atmos. Environ., 45, 2284–2296, https://doi.org/10.1016/j.atmosenv.2010.11.045, 2011.

Baig, S., Medlyn, B. E., Mercado, L. M., and Zaehle, S.: Does the growth response of woody plants to elevated CO_2 increase with temperature? A model-oriented meta-analysis, Glob. Change Biol., 21, 4303–4319, https://doi.org/10.1111/gcb.12962, 2015.

Bellamy, P. H., Loveland, P. J., Bradley, R. I., Lark, R. M., and Kirk, G. J.: Carbon losses from all soils across England and Wales 1978–2003, Nature, 437, 245–248, 2005.

Bernacchi, C. J., Calfapietra, C., Davey, P. A., Wittig, V. E., Scarascia-Mugnozza, G. E., Raines, C. A., and Long, S. P.: Photosynthesis and stomatal conductance responses of poplars to free-air CO_2 enrichment (PopFACE) during the first growth cycle and immediately following coppice., New Phytol., 159, 609–621, 2003.

Best, M. J., Pryor, M., Clark, D. B., Rooney, G. G., Essery, R. L. H., Ménard, C. B., Edwards, J. M., Hendry, M. A., Porson, A., Gedney, N., Mercado, L. M., Sitch, S., Blyth, E., Boucher, O., Cox, P. M., Grimmond, C. S. B., and Harding, R. J.: The Joint UK Land Environment Simulator (JULES), model description – Part 1: Energy and water fluxes, Geosci. Model Dev., 4, 677–699, https://doi.org/10.5194/gmd-4-677-2011, 2011.

Betts, R. A., Boucher, O., Collins, M., Cox, P. M., Falloon, P. D., Gedney, N., Hemming, D. L., Huntingford, C., Jones, C. D., and Sexton, D. M.: Projected increase in continental runoff due to plant responses to increasing carbon dioxide, Nature, 448, 1037–1041, 2007.

Boden, T. A., Marland, G., and Andres, R. J.: Global, Regional, and National Fossil-Fuel CO_2 Emissions, Oak Ridge National Laboratory, U.S. Department of Energy, Oak Ridge, Tenn., USA, 2013.

Büker, P., Feng, Z., Uddling, J., Briolat, A., Alonso, R., Braun, S., Elvira, S., Gerosa, G., Karlsson, P. E., Le Thiec, D., Marzuoli, R., Mills, G., Oksanen, E., Wieser, G., Wilkinson, M., and Emberson, L. D.: New flux based dose-response relationships for ozone for European forest tree species, Environ. Pollut., 206, 163–174, 2015.

Calvete-Sogo, H., Elvira, S., Sanz, J., González-Fernández, I., García-Gómez, H., Sánchez-Martín, L., Alonso, R., and Bermejo-Bermejo, V.: Current ozone levels threaten gross primary production and yield of Mediterranean annual pastures and nitrogen modulates the response, Atmos. Environ., 95, 197–206, https://doi.org/10.1016/j.atmosenv.2014.05.073, 2014.

Capriel, P.: Trends in organic carbon and nitrogen contents in agricultural soils in Bavaria (south Germany) between 1986 and 2007, Euro. J. Soil Sci., 64, 445–454, 2013.

Cech, P. G., Pepin, S., and Korner, C.: Elevated CO_2 reduces sap flux in mature deciduous forest trees, Oecologia, 137, 258–268, 2003.

Ceulemans, R. and Mousseau, M.: Effects of elevated atmospheric CO_2 on woody plants, New Phytol., 127, 425–446, 1994.

Ciais, P., Wattenbach, M., Vuichard, N., Smith, P., Piao, S., Don, A., Luyssaert, S., Janssens, I., Bondeau, A., and Dechow, R.: The European carbon balance, Part 2: croplands, Glob. Change Biol., 16, 1409–1428, 2010.

Ciais, P., Sabine, C., Bala, G., Bopp, L., Brovkin, V., Canadell, J., Chhabra, A., DeFries, R., Galloway, J., Heimann, M., Jones, C., Le Quéré, C., Myneni, R. B., Piao, S., and Thornton, P.: Carbon and Other Biogeochemical Cycles, In: Climate Change 2013: The Physical Science Basis, Contribution of Working Group I to the Fifth Assessment Report of the Intergovernmental Panel on Climate Change, edited by: Stocker, T. F., Qin, D., Plattner, G.-K., Tignor, M., Allen, S. K., Boschung, J., Nauels, A., Xia, Y., Bex, V., and Midgley, P. M., Cambridge University Press, Cambridge, United Kingdom and New York, NY, USA, 2013.

Clark, D. B., Mercado, L. M., Sitch, S., Jones, C. D., Gedney, N., Best, M. J., Pryor, M., Rooney, G. G., Essery, R. L. H., Blyth, E., Boucher, O., Harding, R. J., Huntingford, C., and Cox, P. M.: The Joint UK Land Environment Simulator (JULES), model description – Part 2: Carbon fluxes and vegetation dynamics, Geosci. Model Dev., 4, 701–722, https://doi.org/10.5194/gmd-4-701-2011, 2011.

CLRTAP: The UNECE Convention on Long-range Transboundary Air Pollution, Manual on Methodologies and Criteria for Modelling and Mapping Critical Loads and Levels and Air Pollution Effects, Risks and Trends: Chapter III Mapping Critical Levels for Vegetation, available at: http://icpvegetation.ceh.ac.uk/publications/documents/Chapter3-MappingcriticallevelsforvegetationDOT000.pdf (last access: 15 March 2018), 2017.

Collins, W. J., Sitch, S., and Boucher, O.: How vegetation impacts affect climate metrics for ozone precursors, J. Geophys. Res.-Atmos., 115, D23308, https://doi.org/10.1029/2010JD014187, 2010.

Collins, W. J., Bellouin, N., Doutriaux-Boucher, M., Gedney, N., Halloran, P., Hinton, T., Hughes, J., Jones, C. D., Joshi, M., Liddicoat, S., Martin, G., O'Connor, F., Rae, J., Senior, C., Sitch, S., Totterdell, I., Wiltshire, A., and Woodward, S.: Development and evaluation of an Earth-System model – HadGEM2, Geosci. Model Dev., 4, 1051–1075, https://doi.org/10.5194/gmd-4-1051-2011, 2011.

Cooper, O. R., Parrish, D. D., Stohl, A., Trainer, M., Nedelec, P., Thouret, V., Cammas, J. P., Oltmans, S. J., Johnson, B. J., Tarasick, D., Leblanc, T., McDermid, I. S., Jaffe, D., Gao, R., Stith, J., Ryerson, T., Aikin, K., Campos, T., Weinheimer, A., and Avery, M. A.: Increasing springtime ozone mixing ratios in the free troposphere over western North America, Nature, 463, 344–348, 2010.

Cooper, O. R., Parrish, D., Ziemke, J., Balashov, N., Cupeiro, M., Galbally, I., Gilge, S., Horowitz, L., Jensen, N., and Lamarque, J.-F.: Global distribution and trends of tropospheric ozone: An observation-based review, Elementa, 2, 000029, https://doi.org/10.12952/journal.elementa.000029, 2014.

Cox, P. M., Betts, R. A., Jones, C. D., Spall, S. A., and Totterdell, I. J.: Acceleration of global warming due to carbon-cycle feedbacks in a coupled climate model, Nature, 408, 184–187, 2000.

Cox, P. M.: Description of the TRIFFID dynamic global vegetation model, Hadley Centre technical note 24, 2001.

Cruz, F. T., Pitman, A. J., and Wang, Y. P.: Can the stomatal response to higher atmospheric carbon dioxide explain the unusual temperatures during the 2002 Murray-Darling Basin drought?, J. Geophys. Res.-Atmos., 115, D02101, https://doi.org/10.1029/2009JD012767, 2010.

de Arellano, J. V.-G., van Heerwaarden, C. C., and Lelieveld, J.: Modelled suppression of boundary-layer clouds by plants in a CO_2-rich atmosphere, Nat. Geosci., 5, 701–704, 2012.

De Kauwe, M. G., Kala, J., Lin, Y.-S., Pitman, A. J., Medlyn, B. E., Duursma, R. A., Abramowitz, G., Wang, Y.-P., and Miralles, D. G.: A test of an optimal stomatal conductance scheme within the CABLE land surface model, Geosci. Model Dev., 8, 431–452, https://doi.org/10.5194/gmd-8-431-2015, 2015.

Derwent, R. G., Stevenson, D. S., Doherty, R. M., Collins, W. J., Sanderson, M. G., and Johnson, C. E.: Radiative forcing from surface NO_x emissions: spatial and seasonal variations, Climatic

Change, 88, 385–401, https://doi.org/10.1007/s10584-007-9383-8, 2008.

Derwent, R. G., Utembe, S. R., Jenkin, M. E., and Shallcross, D. E.: Tropospheric ozone production regions and the intercontinental origins of surface ozone over Europe, Atmos. Environ., 112, 216–224, https://doi.org/10.1016/j.atmosenv.2015.04.049, 2015.

Ellsworth, D. S.: CO_2 enrichment in a maturing pine forest: are CO_2 exchange and water status in the canopy affected?, Plant Cell Environ., 22, 461–472, 1999.

Emberson, L. D., Ashmore, M. R., Cambridge, H. M., Simpson, D., and Tuovinen, J.-P.: Modelling stomatal ozone flux across Europe, Environ. Pollut., 109, 403–413, 2000.

Emberson, L. D., Simpson, D., Tuovinen, J.-P., Ashmore, M. R., and Cambridge, H. M.: Modelling and mapping ozone deposition in Europe, Water Air Soil Poll., 130, 577–582, 2001.

Emberson, L. D., Büker, P., and Ashmore, M. R.: Assessing the risk caused by ground level ozone to European forest trees: A case study in pine, beech and oak across different climate regions, Environ. Pollut., 147, 454–466, 2007.

Engardt, M., Simpson, D., Schwikowski, M., and Granat, L.: Deposition of sulphur and nitrogen in Europe 1900–2050, Model calculations and comparison to historical observations, Tellus B, 69, 1328945, https://doi.org/10.1080/16000889.2017.1328945, 2017.

Etheridge, D. M., Steele, L. P., Langenfelds, R. L., Francey, R. J., Barnola, J. M., and Morgan, V. I.: Natural and anthropogenic changes in atmospheric CO_2 over the last 1000 years from air in Antarctic ice and firn, J. Geophys. Res., 101, 4115–4128, https://doi.org/10.1029/95JD03410, 1996.

Fagnano, M., Maggio, A., and Fumagalli, I.: Crops' responses to ozone in Mediterranean environments, Environ. Pollut., 157, 1438–1444, 2009.

Fares, S., Vargas, R., Detto, M., Goldstein, A. H., Karlik, J., Paoletti, E., and Vitale, M.: Tropospheric ozone reduces carbon assimilation in trees: estimates from analysis of continuous flux measurements, Glob. Change Biol., 19, 2427–2443, 2013.

Felzer, B., Reilly, J., Melillo, J., Kicklighter, D., Sarofim, M., Wang, C., Prinn, R., and Zhuang, Q.: Future Effects of Ozone on Carbon Sequestration and Climate Change Policy Using a Global Biogeochemical Model, Climatic Change, 73, 345–373, https://doi.org/10.1007/s10584-005-6776-4, 2005.

Felzer, B. S. F., Kicklighter, D. W., Melillo, J. M., Wang, C., Zhuang, Q., and Prinn, R. G.: Ozone effects on net primary productivity and carbon sequestration in the conterminous United States using a biogeochemistry model, Tellus, 56B, 230–248, 2004.

Feng, Z., Kobayashi, K., and Ainsworth, E. A.: Impact of elevated ozone concentration on growth, physiology, and yield of wheat (Triticum aestivum L.): a meta-analysis, Glob. Change Biol., 14, 2696–2708, https://doi.org/10.1111/j.1365-2486.2008.01673.x, 2008.

Fowler, D., Flechard, C., Cape, J. N., Storeton-West, R. L., and Coyle, M.: Measurements of Ozone Deposition to Vegetation Quantifying the Flux, the Stomatal and Non-Stomatal Components, Water Air Soil Poll., 130, 63–74, https://doi.org/10.1023/a:1012243317471, 2001.

Fowler, D., Pilegaard, K., Sutton, M., Ambus, P., Raivonen, M., Duyzer, J., Simpson, D., Fagerli, H., Fuzzi, S., and Schjørring, J. K.: Atmospheric composition change: ecosystems–atmosphere interactions, Atmos. Environ., 43, 5193–5267, 2009.

Franz, M., Simpson, D., Arneth, A., and Zaehle, S.: Development and evaluation of an ozone deposition scheme for coupling to a terrestrial biosphere model, Biogeosciences, 14, 45–71, https://doi.org/10.5194/bg-14-45-2017, 2017.

Friedlingstein, P., Cox, P., Betts, R., Bopp, L., von Bloh, W., Brovkin, V., Cadule, P., Doney, S., Eby, M., Fung, I., Bala, G., John, J., Jones, C., Joos, F., Kato, T., Kawamiya, M., Knorr, W., Lindsay, K., Matthews, H. D., Raddatz, T., Rayner, P., Reick, C., Roeckner, E., Schnitzler, K. G., Schnur, R., Strassmann, K., Weaver, A. J., Yoshikawa, C., and Zeng, N.: Climate–Carbon Cycle Feedback Analysis: Results from the C4MIP Model Intercomparison, J. Climate, 19, 3337–3353, https://doi.org/10.1175/jcli3800.1, 2006.

Fuhrer, J., Val Martin, M., Mills, G., Heald, C. L., Harmens, H., Hayes, F., Sharps, K., Bender, J., and Ashmore, M. R.: Current and future ozone risks to global terrestrial biodiversity and ecosystem processes, Ecol. Evol., 6, 8785–8799, https://doi.org/10.1002/ece3.2568, 2016.

Gedney, N., Cox, P. M., Bett, R. A., Boucher, O., Huntingford, C., and Stott, P. A.: Detection of a direct carbon dioxide effect in continental river runoff records, Nature, 439, 835–838, 2006.

Gerosa, G., Marzuoli, R., Monteleone, B., Chiesa, M., and Finco, A.: Vertical Ozone Gradients above Forests, Comparison of Different Calculation Options with Direct Ozone Measurements above a Mature Forest and Consequences for Ozone Risk Assessment, Forests, 8, 337, https://doi.org/10.3390/f8090337, 2017.

Grantz, D., Gunn, S., and VU, H. B.: O_3 impacts on plant development: a meta-analysis of root/shoot allocation and growth, Plant Cell Environ., 29, 1193–1209, 2006.

Harmens, H., Mills, G., Emberson, L. D., and Ashmore, M. R.: Implications of climate change for the stomatal flux of ozone: A case study for winter wheat, Environ. Pollut., 146, 763–770, https://doi.org/10.1016/j.envpol.2006.05.018, 2007.

Hayes, F., Wagg, S., Mills, G., Wilkinson, S., and Davies, W.: Ozone effects in a drier climate: implications for stomatal fluxes of reduced stomatal sensitivity to soil drying in a typical grassland species, Glob. Change Biol., 18, 948–959, 2012.

Heikkinen, J., Ketoja, E., Nuutinen, V., and Regina, K.: Declining trend of carbon in Finnish cropland soils in 1974–2009, Glob. Change Biol., 19, 1456–1469, https://doi.org/10.1111/gcb.12137, 2013.

Hofmockel, K. S., Zak, D. R., Moran, K. K., and Jastrow, J. D.: Changes in forest soil organic matter pools after a decade of elevated CO_2 and O_3, Soil Biol. Biochem., 43, 1518–1527, https://doi.org/10.1016/j.soilbio.2011.03.030, 2011.

Hoshika, Y., Watanabe, M., Inada, N., and Koike, T.: Ozone-induced stomatal sluggishness develops progressively in Siebold's beech (Fagus crenata), Environ. Pollut., 166, 152–156, 2012a.

Hoshika, Y., Omasa, K., and Paoletti, E.: Whole-Tree Water Use Efficiency Is Decreased by Ambient Ozone and Not Affected by O_3-Induced Stomatal Sluggishness, Plos One, 7, e39270, https://doi.org/10.1371/journal.pone.0039270, 2012b.

Hoshika, Y., Watanabe, M., Inada, N., and Koike, T.: Model-based analysis of avoidance of ozone stress by stomatal closure in Siebold's beech (*Fagus crenata*), Ann. Bot.-London, 112, 1149–1158, 2013.

Hoshika, Y., Katata, G., Deushi, M., Watanabe, M., Koike, T., and Paoletti, E.: Ozone-induced stomatal sluggishness changes carbon and water balance of temperate deciduous forests, Sci. Rep., 9871, https://doi.org/10.1038/srep09871, 2015.

Hurtt, G., Chini, L. P., Frolking, S., Betts, R., Feddema, J., Fischer, G., Fisk, J., Hibbard, K., Houghton, R., Janetos, A., and Jones, C. D.: Harmonization of land-use scenarios for the period 1500–2100: 600 years of global gridded annual land-use transitions, wood harvest, and resulting secondary lands, Climatic Change, 109, 117–161, 2011.

IGBP-DIS: International Geosphere-Biosphere Programme, Data and Information System, Potsdam, Germany, available from Oak Ridge National Laboratory Distributed Active Archive Center, Oak Ridge, TN, available at: https://daac.ornl.gov/, last access: April 2015.

IPCC: Climate change 2013: The Physical Science Basis, IPCC Working Group I Contribution to AR5, 2013.

Jacobs, C. M. J.: Direct impact of atmospheric CO_2 enrichment on regional transpiration, Wageningen Agricultural University, the Netherlands, 1994.

Janssens, I. A., Freibauer, A., Ciais, P., Smith, P., Nabuurs, G.-J., Folberth, G., Schlamadinger, B., Hutjes, R. W. A., Ceulemans, R., Schulze, E.-D., Valentini, R., and Dolman, A. J.: Europe's Terrestrial Biosphere Absorbs 7 to 12 % of European Anthropogenic CO_2 Emissions, Science, 300, 1538–1542, https://doi.org/10.1126/science.1083592, 2003.

Jones, C. D., Cox, P., and Huntingford, C.: Uncertainty in climate–arbon-cycle projections associated with the sensitivity of soil respiration to temperature, Tellus B, 55, 642–648, https://doi.org/10.1034/j.1600-0889.2003.01440.x, 2003.

Jung, M., Reichstein, M., Margolis, H. A., Cescatti, A., Richardson, A. D., Arain, M. A., Arneth, A., Bernhofer, C., Bonal, D., Chen, J., Gianelle, D., Gobron, N., Kiely, G., Kutsch, W., Lasslop, G., Law, B. E., Lindroth, A., Merbold, L., Montagnani, L., Moors, E. J., Papale, D., Sottocornola, M., Vaccari, F., and Williams, C.: Global patterns of land-atmosphere fluxes of carbon dioxide, latent heat, and sensible heat derived from eddy covariance, satellite, and meteorological observations, J. Geophys. Res.-Biogeo., 116, G00J07, https://doi.org/10.1029/2010JG001566, 2011.

Kala, J., De Kauwe, M. G., Pitman, A. J., Medlyn, B. E., Wang, Y. P., Lorenz, R., and Perkins-Kirkpatrick, S. E.: Impact of the representation of stomatal conductance on model projections of heatwave intensity, Sci. Rep., 1–7, 23418, https://doi.org/10.1038/srep23418, 2016.

Karlsson, P. E., Braun, S., Broadmeadow, M., Elvira, S., Emberson, L., Gimeno, B. S., Le Thiec, D., Novak, K., Oksanen, E., Schaub, M., Uddling, J., and Wilkinson, M.: Risk assessments for forest trees: The performance of the ozone flux versus the AOT concepts, Environ. Pollut., 146, 608–616, https://doi.org/10.1016/j.envpol.2006.06.012, 2007.

Karnosky, D., Percy, K. E., Xiang, B., Callan, B., Noormets, A., Mankovska, B., Hopkin, A., Sober, J., Jones, W., and Dickson, R.: Interacting elevated CO_2 and tropospheric O_3 predisposes aspen (Populus tremuloides Michx.) to infection by rust (Melampsora medusae f. sp. tremuloidae), Glob. Change Biol., 8, 329–338, 2002.

Karnosky, D. F., Skelly, J. M., Percy, K. E., and Chappelka, A. H.: Perspectives regarding 50 years of research on effects of tropospheric ozone air pollution on US forests, Environ. Pollut., 147, 489–506, 2007.

Keeling, C. D. and Whorf, T. P.: Atmospheric CO_2 records from sites in the SIO air sampling network. In Trends: A Compendium of Data on Global Change, Carbon Dioxide Information Analysis Center, Oak Ridge National Laboratory, Oak Ridge, Tenn., USA, 2004.

Kitao, M., Löw, M., Heerdt, C., Grams, T. E., Häberle, K.-H., and Matyssek, R.: Effects of chronic elevated ozone exposure on gas exchange responses of adult beech trees (Fagus sylvatica) as related to the within-canopy light gradient, Environ. Pollut., 157, 537–544, 2009.

Kjellström, E., Nikulin, G., Hansson, U., Strandberg, G., and Ullerstig, A.: 21st century changes in the European climate: uncertainties derived from an ensemble of regional climate model simulations, Tellus A, 63, 24–40, 2011.

Kubiske, M., Quinn, V., Marquardt, P., and Karnosky, D.: Effects of Elevated Atmospheric CO_2 and/or O_3 on Intra-and Interspecific Competitive Ability of Aspen, Plant Biol., 9, 342–355, 2007.

Lamarque, J.-F., Shindell, D. T., Josse, B., Young, P. J., Cionni, I., Eyring, V., Bergmann, D., Cameron-Smith, P., Collins, W. J., Doherty, R., Dalsoren, S., Faluvegi, G., Folberth, G., Ghan, S. J., Horowitz, L. W., Lee, Y. H., MacKenzie, I. A., Nagashima, T., Naik, V., Plummer, D., Righi, M., Rumbold, S. T., Schulz, M., Skeie, R. B., Stevenson, D. S., Strode, S., Sudo, K., Szopa, S., Voulgarakis, A., and Zeng, G.: The Atmospheric Chemistry and Climate Model Intercomparison Project (ACCMIP): overview and description of models, simulations and climate diagnostics, Geosci. Model Dev., 6, 179–206, https://doi.org/10.5194/gmd-6-179-2013, 2013.

Langner, J., Engardt, M., Baklanov, A., Christensen, J. H., Gauss, M., Geels, C., Hedegaard, G. B., Nuterman, R., Simpson, D., Soares, J., Sofiev, M., Wind, P., and Zakey, A.: A multi-model study of impacts of climate change on surface ozone in Europe, Atmos. Chem. Phys., 12, 10423–10440, https://doi.org/10.5194/acp-12-10423-2012, 2012a.

Langner, J., Engardt, M., and Andersson, C.: European summer surface ozone 1990–2100, Atmos. Chem. Phys., 12, 10097–10105, https://doi.org/10.5194/acp-12-10097-2012, 2012b.

Le Quéré, C., Moriarty, R., Andrew, R. M., Peters, G. P., Ciais, P., Friedlingstein, P., Jones, S. D., Sitch, S., Tans, P., Arneth, A., Boden, T. A., Bopp, L., Bozec, Y., Canadell, J. G., Chini, L. P., Chevallier, F., Cosca, C. E., Harris, I., Hoppema, M., Houghton, R. A., House, J. I., Jain, A. K., Johannessen, T., Kato, E., Keeling, R. F., Kitidis, V., Klein Goldewijk, K., Koven, C., Landa, C. S., Landschützer, P., Lenton, A., Lima, I. D., Marland, G., Mathis, J. T., Metzl, N., Nojiri, Y., Olsen, A., Ono, T., Peng, S., Peters, W., Pfeil, B., Poulter, B., Raupach, M. R., Regnier, P., Rödenbeck, C., Saito, S., Salisbury, J. E., Schuster, U., Schwinger, J., Séférian, R., Segschneider, J., Steinhoff, T., Stocker, B. D., Sutton, A. J., Takahashi, T., Tilbrook, B., van der Werf, G. R., Viovy, N., Wang, Y.-P., Wanninkhof, R., Wiltshire, A., and Zeng, N.: Global carbon budget 2014, Earth Syst. Sci. Data, 7, 47–85, https://doi.org/10.5194/essd-7-47-2015, 2015.

Le Quéré, C., Andrew, R. M., Canadell, J. G., Sitch, S., Korsbakken, J. I., Peters, G. P., Manning, A. C., Boden, T. A., Tans, P. P., Houghton, R. A., Keeling, R. F., Alin, S., Andrews, O. D., Anthoni, P., Barbero, L., Bopp, L., Chevallier, F., Chini, L. P., Ciais, P., Currie, K., Delire, C., Doney, S. C., Friedlingstein, P.,

Gkritzalis, T., Harris, I., Hauck, J., Haverd, V., Hoppema, M., Klein Goldewijk, K., Jain, A. K., Kato, E., Körtzinger, A., Landschützer, P., Lefèvre, N., Lenton, A., Lienert, S., Lombardozzi, D., Melton, J. R., Metzl, N., Millero, F., Monteiro, P. M. S., Munro, D. R., Nabel, J. E. M. S., Nakaoka, S.-I., O'Brien, K., Olsen, A., Omar, A. M., Ono, T., Pierrot, D., Poulter, B., Rödenbeck, C., Salisbury, J., Schuster, U., Schwinger, J., Séférian, R., Skjelvan, I., Stocker, B. D., Sutton, A. J., Takahashi, T., Tian, H., Tilbrook, B., van der Laan-Luijkx, I. T., van der Werf, G. R., Viovy, N., Walker, A. P., Wiltshire, A. J., and Zaehle, S.: Global Carbon Budget 2016, Earth Syst. Sci. Data, 8, 605–649, https://doi.org/10.5194/essd-8-605-2016, 2016.

Le Quéré, C., Andrew, R. M., Friedlingstein, P., Sitch, S., Pongratz, J., Manning, A. C., Korsbakken, J. I., Peters, G. P., Canadell, J. G., Jackson, R. B., Boden, T. A., Tans, P. P., Andrews, O. D., Arora, V. K., Bakker, D. C. E., Barbero, L., Becker, M., Betts, R. A., Bopp, L., Chevallier, F., Chini, L. P., Ciais, P., Cosca, C. E., Cross, J., Currie, K., Gasser, T., Harris, I., Hauck, J., Haverd, V., Houghton, R. A., Hunt, C. W., Hurtt, G., Ilyina, T., Jain, A. K., Kato, E., Kautz, M., Keeling, R. F., Klein Goldewijk, K., Körtzinger, A., Landschützer, P., Lefèvre, N., Lenton, A., Lienert, S., Lima, I., Lombardozzi, D., Metzl, N., Millero, F., Monteiro, P. M. S., Munro, D. R., Nabel, J. E. M. S., Nakaoka, S.-I., Nojiri, Y., Padin, X. A., Peregon, A., Pfeil, B., Pierrot, D., Poulter, B., Rehder, G., Reimer, J., Rödenbeck, C., Schwinger, J., Séférian, R., Skjelvan, I., Stocker, B. D., Tian, H., Tilbrook, B., Tubiello, F. N., van der Laan-Luijkx, I. T., van der Werf, G. R., van Heuven, S., Viovy, N., Vuichard, N., Walker, A. P., Watson, A. J., Wiltshire, A. J., Zaehle, S., and Zhu, D.: Global Carbon Budget 2017, Earth Syst. Sci. Data, 10, 405–448, https://doi.org/10.5194/essd-10-405-2018, 2018.

Leuzinger, S. and Körner, C.: Water savings in mature deciduous forest trees under elevated CO_2, Glob. Change Biol., 13, 2498–2508, https://doi.org/10.1111/j.1365-2486.2007.01467.x, 2007.

Lin, Y.-S., Medlyn, B. E., Duursma, R. A., Prentice, I. C., Wang, H., Baig, S., Eamus, D., de Dios, V. R., Mitchell, P., and Ellsworth, D. S.: Optimal stomatal behaviour around the world, Nat. Clim. Change, 5, 459–464, 2015.

Lindroth, R. L.: Impacts of Elevated Atmospheric CO_2 and O_3 on Forests: Phytochemistry, Trophic Interactions, and Ecosystem Dynamics, J. Chem. Ecol., 36, 2–21, https://doi.org/10.1007/s10886-009-9731-4, 2010.

Logan, J. A., Staehelin, J., Megretskaia, I. A., Cammas, J. P., Thouret, V., Claude, H., De Backer, H., Steinbacher, M., Scheel, H. E., Stübi, R., Fröhlich, M., and Derwent, R.: Changes in ozone over Europe: Analysis of ozone measurements from sondes, regular aircraft (MOZAIC) and alpine surface sites, J. Geophys. Res., 117, 1–23, 2012.

Lombardozzi, D., Levis, S., Bonan, G., and Sparks, J. P.: Predicting photosynthesis and transpiration responses to ozone: decoupling modeled photosynthesis and stomatal conductance, Biogeosciences, 9, 3113–3130, https://doi.org/10.5194/bg-9-3113-2012, 2012.

Lombardozzi, D., Levis, S., Bonan, G., Hess, P. G., and Sparks, J. P.: The Influence of Chronic Ozone Exposure on Global Carbon and Water Cycles, J. Climate, 28, 292–305, https://doi.org/10.1175/jcli-d-14-00223.1, 2015.

Long, S. P., Ainsworth, E. A., Leakey, A. D. B., Nosberger, J., and Ort, D. R.: Food for Thought: Lower-Than-Expected Crop Yield Stimulation with Rising CO_2 Concentrations, Science, 312, 1918–1921, https://doi.org/10.1126/science.1114722, 2006.

Löw, M., Herbinger, K., Nunn, A., Häberle, K.-H., Leuchner, M., Heerdt, C., Werner, H., Wipfler, P., Pretzsch, H., and Tausz, M.: Extraordinary drought of 2003 overrules ozone impact on adult beech trees (Fagus sylvatica), Trees, 20, 539–548, 2006.

Loya, W. M., Pregitzer, K. S., Karberg, N. J., King, J. S., and Giardina, C. P.: Reduction of soil carbon formation by tropospheric ozone under increased carbon dioxide levels, Nature, 425, 705–707, 2003.

Luyssaert, S., Abril, G., Andres, R., Bastviken, D., Bellassen, V., Bergamaschi, P., Bousquet, P., Chevallier, F., Ciais, P., Corazza, M., Dechow, R., Erb, K.-H., Etiope, G., Fortems-Cheiney, A., Grassi, G., Hartmann, J., Jung, M., Lathière, J., Lohila, A., Mayorga, E., Moosdorf, N., Njakou, D. S., Otto, J., Papale, D., Peters, W., Peylin, P., Raymond, P., Rödenbeck, C., Saarnio, S., Schulze, E.-D., Szopa, S., Thompson, R., Verkerk, P. J., Vuichard, N., Wang, R., Wattenbach, M., and Zaehle, S.: The European land and inland water CO_2, CO, CH_4 and N_2O balance between 2001 and 2005, Biogeosciences, 9, 3357–3380, https://doi.org/10.5194/bg-9-3357-2012, 2012.

Massman, W. J.: A review of the molecular diffusivities of H_2O, CO_2, CH_4, CO, O_3, SO_2, NH_3, N_2O, NO, and NO_2 in air, O_2 and N_2 near STP, Atmos. Environ., 32, 1111–1127, https://doi.org/10.1016/S1352-2310(97)00391-9, 1998.

Matyssek, R., Wieser, G., Ceulemans, R., Rennenberg, H., Pretzsch, H., Haberer, K., Löw, M., Nunn, A., Werner, H., and Wipfler, P.: Enhanced ozone strongly reduces carbon sink strength of adult beech (Fagus sylvatica) – Resume from the free-air fumigation study at Kranzberg Forest, Environ. Pollut., 158, 2527–2532, 2010a.

Matyssek, R., Karnosky, D., Wieser, G., Percy, K., Oksanen, E., Grams, T., Kubiske, M., Hanke, D., and Pretzsch, H.: Advances in understanding ozone impact on forest trees: messages from novel phytotron and free-air fumigation studies, Environ. Pollut., 158, 1990–2006, 2010b.

McLaughlin, S. B., Nosal, M., Wullschleger, S. D., and Sun, G.: Interactive effects of ozone and climate on tree growth and water use in a southern Appalachian forest in the USA, New Phytol., 174, 109–124, https://doi.org/10.1111/j.1469-8137.2007.02018.x, 2007a.

McLaughlin, S. B., Wullschleger, S. D., Sun, G., and Nosal, M.: Interactive effects of ozone and climate on water use, soil moisture content and streamflow in a southern Appalachian forest in the USA, New Phytol., 174, 125–136, https://doi.org/10.1111/j.1469-8137.2007.01970.x, 2007b.

Medlyn, B. E., Badeck, F. W., De Pury, D. G. G., Barton, C. V. M., Broadmeadow, M., Ceulemans, R., De Angelis, P., Forstreuter, M., Jach, M. E., Kellomaki, S., Laitat, E., Marek, M., Philippot, S., Rey, A., Strassemeyer, J., Laitinen, K., Liozon, R., Portier, B., Roberntz, P., Wang, K., and Jstbid, P. G.: Effects of elevated $[CO_2]$ on photosynthesis in European forest species: a meta-analysis of model parameters, Plant Cell Environ., 22, 1475–1495, https://doi.org/10.1046/j.1365-3040.1999.00523.x, 1999.

Medlyn, B. E., Barton, C. V. M., Broadmeadow, M. S. J., Ceulemans, R., De Angelis, P., Forstreuter, M., Freeman, M., Jackson, S. B., Kellomaki, S., Laitat, E., Rey, A., Roberntz, P., Sigurdsson, B. D., Strassemeyer, J., Wang, K., Curtis, P. S., and Jarvis, P. G.: Stomatal conductance of forest species after long-term ex-

posure to elevated CO_2 concentration: a synthesis, New Phytol., 149, 247–264, 2001.

Medlyn, B. E., Duursma, R. A., Eamus, D., Ellsworth, D. S., Prentice, I. C., Barton, C. V., Crous, K. Y., de Angelis, P., Freeman, M., and Wingate, L.: Reconciling the optimal and empirical approaches to modelling stomatal conductance, Glob. Change Biol., 17, 2134–2144, 2011.

Mercado, L. M., Bellouin, N., Sitch, S., Boucher, O., Huntingford, C., Wild, M., and Cox, P. M.: Impact of changes in diffuse radiation on the global land carbon sink, Nature, 458, 1014–1017, 2009.

Mills, G., Hayes, F., Wilkinson, S., and Davies, W. J.: Chronic exposure to increasing background ozone impairs stomatal functioning in grassland species, Glob. Change Biol., 15, 1522–1533, 2009.

Mills, G., Pleijel, H., Braun, S., Büker, P., Bermejo, V., Calvo, E., Danielsson, H., Emberson, L., Grünhage, L., Fernández, I. G., Harmens, H., Hayes, F., Karlsson, P.-E., and Simpson, D.: New stomatal flux-based critical levels for ozone effects on vegetation, Atmos. Environ., 45, 5064–5068, 2011a.

Mills, G., Hayes, F., Simpson, D., Emberson, L., Norris, D., Harmens, H., and BÜKer, P.: Evidence of widespread effects of ozone on crops and (semi-)natural vegetation in Europe (1990–2006) in relation to AOT40- and flux-based risk maps, Glob. Change Biol., 17, 592–613, https://doi.org/10.1111/j.1365-2486.2010.02217.x, 2011b.

Mills, G., Harmens, H., Wagg, S., Sharps, K., Hayes, F., Fowler, D., Sutton, M., and Davies, B.: Ozone impacts on vegetation in a nitrogen enriched and changing climate, Environ. Pollut., 208, 898–908, 2016.

Norby, R. J., Wullschleger, S. D., Gunderson, C. A., Johnson, D. W., and Ceulemans, R.: Tree responses to rising CO_2 in field experiments: implications for the future forest, Plant Cell Environ., 22, 683–714, 1999.

Norby, R. J., DeLucia, E. H., Gielen, B., Calfapietra, C., Giardina, C. P., King, J. S., Ledford, J., McCarthy, H. R., Moore, D. J. P., Ceulemans, R., De Angelis, P., Finzi, A. C., Karnosky, D. F., Kubiske, M. E., Lukac, M., Pregitzer, K. S., Scarascia-Mugnozza, G. E., Schlesinger, W. H., and Oren, R.: Forest response to elevated CO_2 is conserved across a broad range of productivity, P. Natl. Acad. Sci. USA, 102, 18052–18056, https://doi.org/10.1073/pnas.0509478102, 2005.

Nunn, A. J., Reiter, I. M., Häberle, K.-H., Langebartels, C., Bahnweg, G., Pretzsch, H., Sandermann, H., and Matyssek, R.: Response patterns in adult forest trees to chronic ozone stress: identification of variations and consistencies, Environ. Pollut., 136, 365–369, 2005.

O'Connor, F. M., Johnson, C. E., Morgenstern, O., Abraham, N. L., Braesicke, P., Dalvi, M., Folberth, G. A., Sanderson, M. G., Telford, P. J., Voulgarakis, A., Young, P. J., Zeng, G., Collins, W. J., and Pyle, J. A.: Evaluation of the new UKCA climate-composition model – Part 2: The Troposphere, Geosci. Model Dev., 7, 41–91, https://doi.org/10.5194/gmd-7-41-2014, 2014.

Paoletti, E. and Grulke, N. E.: Ozone exposure and stomatal sluggishness in different plant physiognomic classes, Environ. Pollut., 158, 2664–2671, 2010.

Parrish, D. D., Law, K. S., Staehelin, J., Derwent, R., Cooper, O. R., Tanimoto, H., Volz-Thomas, A., Gilge, S., Scheel, H.-E., Steinbacher, M., and Chan, E.: Long-term changes in lower tropospheric baseline ozone concentrations at northern mid-latitudes, Atmos. Chem. Phys., 12, 11485–11504, https://doi.org/10.5194/acp-12-11485-2012, 2012.

Parrish, D. D., Law, K. S., Staehelin, J., Derwent, R., Cooper, O. R., Tanimoto, H., Volz-Thomas, A., Gilge, S., Scheel, H. E., Steinbacher, M., and Chan, E.: Lower tropospheric ozone at northern midlatitudes: Changing seasonal cycle, Geophys. Res. Lett., 40, 1631–1636, 2013.

Percy, K. E., Awmack, C. S., Lindroth, R. L., Kubiske, M. E., Kopper, B. J., Isebrands, J., Pregitzer, K. S., Hendrey, G. R., Dickson, R. E., and Zak, D. R.: Altered performance of forest pests under atmospheres enriched by CO_2 and O_3, Nature, 420, 403–407, 2002.

Royal-Society: Ground-level ozone in the 21st century: future trends, impacts and policy implications, Science Policy Report 15/08, 2008.

Samuelsson, P., Jones, C. G., Willén, U., Ullerstig, A., Gollvik, S., Hansson, U., Jansson, C., Kjellström, E., Nikulin, G., and Wyser, K.: The Rossby Centre Regional Climate model RCA3: model description and performance, Tellus A, 63, 4–23, 2011.

Saxe, H., Ellsworth, D. S., and Heath, J.: Tree and forest functioning in an enriched CO_2 atmosphere, New Phytol., 139, 395–436, https://doi.org/10.1046/j.1469-8137.1998.00221.x, 1998.

Schulze, E.-D., Ciais, P., Luyssaert, S., Schrumpf, M., Janssens, I. A., Thiruchittampalam, B., Theloke, J., Saurat, M., Bringezu, S., and Lelieveld, J.: The European carbon balance, Part 4: integration of carbon and other trace-gas fluxes, Glob. Change Biol., 16, 1451–1469, 2010.

Schulze, E. D., Luyssaert, S., Ciais, P., Freibauer, A., Janssens, I. A., et al.: Importance of methane and nitrous oxide for Europe's terrestrial greenhouse-gas balance, Nat. Geosci., 2, 842–850, 2009.

Sicard, P., De Marco, A., Troussier, F., Renoua, C., Vas, N., and Paoletti, E.: Decrease in surface ozone concentrations at Mediterranean remote sites and increase in the cities, Atmos. Environ., 79, 705–715, 2013.

Simpson, D., Benedictow, A., Berge, H., Bergström, R., Emberson, L. D., Fagerli, H., Flechard, C. R., Hayman, G. D., Gauss, M., Jonson, J. E., Jenkin, M. E., Nyíri, A., Richter, C., Semeena, V. S., Tsyro, S., Tuovinen, J.-P., Valdebenito, Á., and Wind, P.: The EMEP MSC-W chemical transport model – technical description, Atmos. Chem. Phys., 12, 7825–7865, https://doi.org/10.5194/acp-12-7825-2012, 2012.

Simpson, D., Andersson, C., Christensen, J. H., Engardt, M., Geels, C., Nyiri, A., Posch, M., Soares, J., Sofiev, M., Wind, P., and Langner, J.: Impacts of climate and emission changes on nitrogen deposition in Europe: a multi-model study, Atmos. Chem. Phys., 14, 6995–7017, https://doi.org/10.5194/acp-14-6995-2014, 2014a.

Simpson, D., Arneth, A., Mills, G., Solberg, S., and Uddling, J.: Ozone – the persistent menace: interactions with the N cycle and climate change, Current Opinion in Environmental Sustainability, 9, 9–19, 2014b.

Sitch, S., Cox, P. M., Collins, W. J., and Huntingford, C.: Indirect radiative forcing of climate change through ozone effects on the land-carbon sink, Nature, 448, 791–794, 2007.

Sitch, S., Friedlingstein, P., Gruber, N., Jones, S. D., Murray-Tortarolo, G., Ahlström, A., Doney, S. C., Graven, H., Heinze, C., Huntingford, C., Levis, S., Levy, P. E., Lomas, M., Poulter, B., Viovy, N., Zaehle, S., Zeng, N., Arneth, A., Bonan,

G., Bopp, L., Canadell, J. G., Chevallier, F., Ciais, P., Ellis, R., Gloor, M., Peylin, P., Piao, S. L., Le Quéré, C., Smith, B., Zhu, Z., and Myneni, R.: Recent trends and drivers of regional sources and sinks of carbon dioxide, Biogeosciences, 12, 653–679, https://doi.org/10.5194/bg-12-653-2015, 2015.

Sleutel, S., De Neve, S., and Hofman, G.: Estimates of carbon stock changes in Belgian cropland, Soil Use Manage., 19, 166–171, https://doi.org/10.1079/SUM2003187, 2003.

Sun, G. E., McLaughlin, S. B., Porter, J. H., Uddling, J., Mulholland, P. J., Adams, M. B., and Pederson, N.: Interactive influences of ozone and climate on streamflow of forested watersheds, Glob. Change Biol., 18, 3395–3409, https://doi.org/10.1111/j.1365-2486.2012.02787.x, 2012.

Tai, P. K. A., Val Martin, M., and Heald, C. L.: Threat to future global food security from climate change and ozone air pollution, Nat. Clim. Change, 4, 817–821, 2014.

Talhelm, A. F., Pregitzer, K. S., Kubiske, M. E., Zak, D. R., Campany, C. E., Burton, A. J., Dickson, R. E., Hendrey, G. R., Isebrands, J. G., Lewin, K. F., Nagy, J., and Karnosky, D. F.: Elevated carbon dioxide and ozone alter productivity and ecosystem carbon content in northern temperate forests, Glob. Change Biol., 20, 2492–2504, https://doi.org/10.1111/gcb.12564, 2014.

Tans, P. and Keeling, R.: NOAA/ESRL (www.esrl.noaa.gov/gmd/ccgg/trends/, last access: January 2017), Scripps Institution of Oceanography (http://scrippsco2.ucsd.edu/, last access: January 2017), 2014.

Tricker, P. J., Pecchiari, M., Bunn, S. M., Vaccari, F. P., Peressotti, A., Miglietta, F., and Taylor, G.: Water use of a bioenergy plantation increases in a future high CO_2 world, Biomass Bioenerg., 33, 200–208, 2009.

Tuovinen, J.-P., Emberson, L., and Simpson, D.: Modelling ozone fluxes to forests for risk assessment: status and prospects, Ann. For. Sci., 66, 1–14, 2009.

Tuovinen, J., Hakola, H., Karlsson, P., and Simpson, D.: Air pollution risks to Northern European forests in a changing climate, Climate Change, Air Pollution and Global Challenges Understanding and Perspectives from Forest Research, in: Understanding and Perspectives from Forest Research, edited by: Matyssek, R., Clarke, N., Cudlin, P., Mikkelsen, T. N., Tuovinen, J.-P., Wieser, G., and Paoletti, E., Elsevier, New York, 2013.

Uddling, J., Teclaw, R. M., Pregitzer, K. S., and Ellsworth, D. S.: Leaf and canopy conductance in aspen and aspen-birch forests under free-air enrichment of carbon dioxide and ozone, Tree Physiol., 29, 1367–1380, 2009.

van Vuuren, D. P., Edmonds, J., Kainuma, M., Riahi, K., Thomson, A., Hibbard, K., Hurtt, G. C., Kram, T., Krey, V., Lamarque, J.-F., Masui, T., Meinshausen, M., Nakicenovic, N., Smith, S. J., and Rose, S. K.: The representative concentration pathways: an overview, Climatic Change, 109, 5–31, https://doi.org/10.1007/s10584-011-0148-z, 2011.

Verstraeten, W. W., Neu, J. L., Williams, J. E., Bowman, K. W., Worden, J. R., and Boersma, K. F.: Rapid increases in tropospheric ozone production and export from China, Nat. Geosci., 8, 690–695, 2015.

Vingarzan, R.: A review of surface ozone background levels and trends, Atmos. Environ., 38, 3431–3442, https://doi.org/10.1016/j.atmosenv.2004.03.030, 2004.

Weedon, G. P., Gomes, S., Viterbo, P., Österle, H., Adam, J. C., Bellouin, N., Boucher, O., and Best, M. J.: The WATCH Forcing Data 1958–2001: a meteorological forcing dataset for land surface- and hydrological models, WATCH Tech. Rep. 22, 41 pp., available at: www.eu-watch.org/publications (last access: May 2014), 2010.

Weedon, G. P., Gomes, S., Viterbo, P., Shuttleworth, W. J., Blyth, E., Österle, H., Adam, J. C., Bellouin, N., Boucher, O., and Best, M.: Creation of the WATCH Forcing data and its use to assess global and regional reference crop evaporation over land during the twentieth century, J. Hydrometeorol., 12, 823–848, https://doi.org/10.1175/2011JHM1369.1, 2011.

Weedon, G. P.: Readme file for the "WFDEI" dataset, available at: http://www.eu-watch.org/gfx_content/documents/README-WFDEI.pdf (last access: May 2014), 2013.

Wild, O.: Modelling the global tropospheric ozone budget: exploring the variability in current models, Atmos. Chem. Phys., 7, 2643–2660, https://doi.org/10.5194/acp-7-2643-2007, 2007.

Wilkinson, S. and Davies, W. J.: Ozone suppresses soil drying-and abscisic acid (ABA)-induced stomatal closure via an ethylene-dependent mechanism, Plant Cell Environ., 32, 949–959, 2009.

Wilkinson, S. and Davies, W. J.: Drought, ozone, ABA and ethylene: new insights from cell to plant to community, Plant Cell Environ., 33, 510–525, https://doi.org/10.1111/j.1365-3040.2009.02052.x, 2010.

Wittig, V. E., Ainsworth, E. A., and Long, S. P.: To what extent do current and projected increases in surface ozone affect photosynthesis and stomatal conductance of trees? A meta-analytic review of the last 3 decades of experiments, Plant Cell Environ., 30, 1150–1162, https://doi.org/10.1111/j.1365-3040.2007.01717.x, 2007.

Wittig, V. E., Ainsworth, E. A., Naidu, S. L., Karnosky, D. F., and Long, S. P.: Quantifying the impact of current and future tropospheric ozone on tree biomass, growth, physiology and biochemistry: a quantitative meta-analysis, Glob. Change Biol., 15, 396–424, https://doi.org/10.1111/j.1365-2486.2008.01774.x, 2009.

Wullschleger, S. D., Gunderson, C. A., Hanson, P. J., Wilson, K. B., and Norby, R. J.: Sensitivity of stomatal and canopy conductance to elevated CO_2 concentration; interacting variables and perspectives of scale, New Phytol., 153, 485–496, https://doi.org/10.1046/j.0028-646X.2001.00333.x, 2002.

Young, P. J., Arneth, A., Schurgers, G., Zeng, G., and Pyle, J. A.: The CO_2 inhibition of terrestrial isoprene emission significantly affects future ozone projections, Atmos. Chem. Phys., 9, 2793–2803, https://doi.org/10.5194/acp-9-2793-2009, 2009.

Young, P. J., Archibald, A. T., Bowman, K. W., Lamarque, J.-F., Naik, V., Stevenson, D. S., Tilmes, S., Voulgarakis, A., Wild, O., Bergmann, D., Cameron-Smith, P., Cionni, I., Collins, W. J., Dalsøren, S. B., Doherty, R. M., Eyring, V., Faluvegi, G., Horowitz, L. W., Josse, B., Lee, Y. H., MacKenzie, I. A., Nagashima, T., Plummer, D. A., Righi, M., Rumbold, S. T., Skeie, R. B., Shindell, D. T., Strode, S. A., Sudo, K., Szopa, S., and Zeng, G.: Pre-industrial to end 21st century projections of tropospheric ozone from the Atmospheric Chemistry and Climate Model Intercomparison Project (ACCMIP), Atmos. Chem. Phys., 13, 2063–2090, https://doi.org/10.5194/acp-13-2063-2013, 2013.

Zaehle, S.: Terrestrial nitrogen-carbon cycle interactions at the global scale, Philos. T. R. Soc. B., 368, 20130125, https://doi.org/10.1098/rstb.2013.0125, 2013.

Zak, D. R., Pregitzer, K. S., Kubiske, M. E., and Burton, A. J.: Forest productivity under elevated CO_2 and O_3: positive feed-

backs to soil N cycling sustain decade-long net primary productivity enhancement by CO_2, Ecol. Lett., 14, 1220–1226, https://doi.org/10.1111/j.1461-0248.2011.01692.x, 2011.